HHS Public Access

Author manuscript

Int Rev Psychiatry. Author manuscript; available in PMC 2018 April 26.

Published in final edited form as:

Int Rev Psychiatry. 2017 April ; 29(2): 115–145. doi:10.1080/09540261.2017.1305949.

The development and modeling of devices and paradigms for transcranial magnetic stimulation

Stefan M. Goetz, PhD and

1-919-613-0322, Duke University, Department of Psychiatry & Behavioral Sciences, Division for Brain Stimulation & Neurophysiology and Department of Electrical & Computer Engineering, Durham, NC 27708

Zhi-De Deng, PhD

1-301-594-0387, National Institutes of Health, National Institute of Mental Health, Intramural Research Program, Experimental Therapeutics & Pathophysiology Branch, Noninvasive Neuromodulation Unit, Bethesda, MD 20892. Duke University, Department of Psychiatry & Behavioral Sciences, Division for Brain Stimulation & Neurophysiology and Duke Institute for Brain Sciences, Durham, NC 27708

Abstract

Magnetic stimulation is a noninvasive neurostimulation technique that can evoke action potentials and modulate neural circuits through induced electric fields. Biophysical models of magnetic stimulation have become a major driver for technological developments and the understanding of the mechanisms of magnetic neurostimulation and neuromodulation. Major technological developments involve stimulation coils with different spatial characteristics and pulse sources to control the pulse waveform. While early technological developments were the result of manual design and invention processes, there is a trend in both stimulation coil and pulse source design to mathematically optimize parameters with the help of computational models. To date, macroscopically highly realistic spatial models of the brain as well as peripheral targets, and user-friendly software packages enable researchers and practitioners to simulate the treatment-specific and induced electric field distribution in the brains of individual subjects and patients. Neuron models further introduce the microscopic level of neural activation to understand the influence of activation dynamics in response to different pulse shapes. A number of models that were designed for online calibration to extract otherwise covert information and biomarkers from the neural system recently form a third branch of modeling.

Keywords

Transcranial magnetic stimulation; TMS; biophysical modeling; neuroscience; neurostimulation; neuromodulation; medical technology

Disclosure of interest

Dr. Deng is an inventor on patents and patent applications related to TMS technology owned by Columbia University. Dr. Deng was supported in part by a grant from the National Institutes of Health / National Center for Advancing Translational Sciences (KL2 TR001115) and by the Intramural Research Program of the National Institute of Mental Health. Dr. Goetz is an inventor on patents and patent applications on technology of transcranial magnetic stimulation. Furthermore, he has received royalties through his current and previous employers as well as patent application support and research funding from Magstim Co.

1 What is TMS and how could modeling improve technology?

Transcranial magnetic stimulation (TMS) is an established method to activate neurons noninvasively in the brain using electromagnetic induction (Barker, Jalinous, & Freeston, 1985; Polson, Barker, & Freeston, 1982). The technique is unmatched in several applications ranging from experimental neuroscience to medical diagnosis and therapy (Aleman, 2013; Eldaief, Press, & Pascual-Leone, 2013; Wassermann & Zimmermann, 2012). Through time-varying current in a stimulation coil, TMS generates strong alternating magnetic field pulses that can permeate the electrically poorly conducting skull and evoke action potentials of neurons in the focus of the stimulation coil. Thus, unlike subthreshold neuromodulation techniques, TMS pulses can trigger a neuron's endogenous signal transmission mechanism, which amplifies the stimulus and transmits the signal to other neurons (Di Lazzaro et al., 2004; Di Lazzaro et al., 2012; Volz, Hamada, Rothwell, & Grefkes, 2014).

However, the interaction of the brain tissue with the electromagnetic fields is not obvious. Accordingly, theoretical and modeling work has accompanied TMS since the invention of this technique (Durand, Ferguson, & Dalbasti, 1989; Guidi, Scarpino, Angeleri, Antili, & Leo, 1989; Lorenzen & Weyh, 1992; Maccabee, Amassian, Cracco, & Cadwell, 1988; McRobbie, 1985; Reilly, 1989; Reilly, 1992; Roth & Basser, 1990; Rudiak & Marg, 1994; Turner, 1986; Ueno, Tashiro, & Harada, 1988a; Yamaguchi et al., 1989). In terms of spatial distribution, the magnetic field that is generated by the current in the stimulation coil is almost independent from the specific head anatomy, whereas the induced electric fields in the brain and around the neurons are not (Esselle & Stuchly, 1992). The induced currents interact with both the macroscopic and microscopic anatomy as well as the varying electrical conductance. Both lead to charge accumulation and influence the distribution of the induced electric field. In terms of the temporal dynamics, neurons have various subtypes, with diverse geometry and membrane excitability, leading to differential response to the current pulse waveforms. The key motivation behind spatial and temporal modeling is to gain a better understanding of the mechanisms of action of TMS, design and optimize devices, and plan as well as guide TMS interventions.

2 What are the physical and physiological fundamentals of TMS?

2.1 Electromagnetism and the spatial aspect of TMS

In contrast to electrical stimulation, where current flows directly between two electrodes, a cathode and an anode, and generates a stimulating electric field, magnetic stimulation uses electromagnetism to induce currents across the skull into the brain without any direct electrical contact. The event chain starts in the stimulation coil, which during a pulse guides a strong alternating current that in turn generates a spatially extended magnetic field. According to Ampère's circuital law, the magnetic field around the coil is proportional to the coil current strength. Although the magnetic field strength decreases rapidly with distance, it reaches into the brain if the coil is placed close enough to a subject's head (Barker, 1991; Deng, Peterchev, & Lisanby, 2008). The alternating nature and briefness of the current pulse and therefore the magnetic field in the brain—which follows the same time course—cause a high time derivative of the magnetic field, i.e., a strong change of the magnetic field over

time (Peterchev, Deng, & Goetz, 2015). According to Faraday's law of induction, the time derivative of the current generates an electric field (Jackson, 1999; Maxwell, 1891).

To this point, the process primarily depends on the coil design, i.e., the shape of the conductors in the coil (see Figs. 2 and 4) as well as potentially implemented magnetically active materials, such as ferromagnetic iron cores (see Figs. 3 and 4), but not on the brain anatomy (Epstein & Davey, 2002; Lorenzen & Weyh, 1992; Tachas & Samaras, 2014). Since the brain is electrically conductive, the induced electric field causes a current that has to follow the brain anatomy and also local electrical conductivity differences caused by different tissue types or tissue compositions according to Ohm's law (Ruohonen et al., 1996; Wagner, Zahn, Grodzinsky, & Pascual-Leone, 2004). At interfaces or gradients between different electrical conductivities, the current transiently builds up charge accumulations, which in turn generate an additional, often called secondary electric field according to Gauss' law. This secondary electric field superimposes the induced electric field and strongly depends on the individual brain anatomy as well as the position of the coil orientation (D'Ostilio et al., 2014; Kammer, Vorwerg, & Herrnberger, 2007; Laakso, Hirata, & Ugawa, 2014; Mills, Boniface, & Schubert, 1992; Opitz, Windhoff, Heidemann, Turner, & Thielscher, 2011; Tofts, 1990). The result of that superposition is the electric field that is considered to cause neural activation in TMS (Esselle & Stuchly, 1992).

The overall process of induction in TMS is described by Maxwell's equations, which summarize the physical laws given above. These equations or derivations thereof are in general the source for all spatial modeling of the electric fields induced by TMS.

2.2 Neurophysiology for the activation process and temporal aspects of TMS

Whereas Maxwell's equations describe the physics of induction, they fall short in describing neural activation. The activation process is in the domain of neurophysiology. Neuron models of various types fill this gap. Neuron models are required, for instance, to estimate the local threshold of activation. For example, neuron models predict that similarly to supra-threshold electrical stimulation the TMS induced electric field may exclusively activate axons as was identified, e.g., by the neural time constant (Corthout, Barker, & Cowey, 2001; D'Ostilio et al., 2016; Nowak & Bullier, 1998a, 1998b; Peterchev, Goetz, Westin, Luber, & Lisanby, 2013). The axonal membrane contains electrically sensitive ion channels, most importantly for the excitation in the brain sodium channels such as $Na_V1.1$, $Na_V1.2$, $Na_V1.3$, and $Na_V1.6$, which respond to electric fields across their structure with nanomechanical conformation changes (Krishnan, Lin, Park, & Kiernan, 2009; Leterrier, Brachet, Dargent, & Vacher, 2011; Trimmer & Rhodes, 2004). The local density and genetic expression of types and subunits depends on both the neuron type and the location (Lai & Jan, 2006; Leterrier, Brachet, Fache, & Dargent, 2010; Trimmer & Rhodes, 2004). The membrane itself behaves electrically as a capacitance (Gentet, Stuart, & Clements, 2000; Howell, Medina, & Grill, 2015). Thus, neuron models are the key to understanding activation dynamics and studying pulse-shape effects. The temporal shape of pulses was reported to substantially affect efficiency and thus coil as well as device heating (Goetz et al., 2013; Goetz, Truong, et al., 2012; Niehaus, Meyer, & Weyh, 2000; Peterchev, Murphy, & Lisanby, 2011), to enable selective activation of certain neuron types or populations (Claus, Murray, Spitzer, & Flügel,

1990; Corthout, et al., 2001; Kammer, Beck, Thielscher, Laubis-Herrmann, & Topka, 2001; Kammer, et al., 2007; Ni et al., 2011; Peterchev, et al., 2013; Sommer, D'Ostilio, et al., 2014), and to increase neuromodulation strength compared to standard biphasic pulses in repetitive protocols (Antal et al., 2002; Arai et al., 2007; Arai et al., 2005; Goetz et al., 2016; Hannah, Ciocca, Sommer, Hammond, & Rothwell, 2014; Sommer, Ciocca, et al., 2014; Sommer, Lang, Tergau, & Paulus, 2002; Sommer et al., 2013). Finally, neuron models also explain and predict directionality effects of TMS, i.e., why the orientation of the coil affects the threshold and allows activation of different neuron populations (Goetz, et al., 2016; Niehaus, et al., 2000).

3 What are the major developments in TMS technology?

Magnetic stimulation devices typically consist of two components: a pulse source that generates the strong rapid current surge during a pulse (Fig. 1A), and a stimulation coil, which is placed over the neural target (Fig. 1B). In available technology, the pulse source determines the temporal shape of a pulse, i.e., the shape of the coil current over time, as well as the temporal sequence of pulse trains. The stimulation coil, on the other hand, is responsible for the spatial distribution of its magnetic field and consequently the spatial distribution of the induced electric field and the current flow in the brain.

3.1 Stimulation coils

3.1.1 Conventional coil designs—The stimulation coil forms the interface of the stimulation system to a subject or patient. Apart from material-related, mechanical, and thermal topics, the fundamental subject of coil design refers to the shape and position of the electrical conductor in the casing to generate a certain magnetic and in turn electric field distribution. As the electric field strength was found to correlate with activation, it should be large in the target area with minimum electric field strength elsewhere (Krings et al., 1997; Opitz et al., 2013). The portfolio of available specialized coils includes devices for small animals, peripheral neural and neuromuscular stimulation, as well as various cortical targets (see Fig. 2) (Bustamante et al., 2013; Bustamante, Gorostiza, López de Santa María Miró, & Iturri, 2007; Crowther et al., 2011; Deng, Lisanby, & Peterchev, 2013; Emrich et al., 2012; Goetz, Afinowi, Herzog, & Weyh, 2013; Goetz, Herzog, Gattinger, & Gleich, 2011; Knäulein & Weyh, 1996; Mueller et al., 2014; Ruohonen, Ravazzani, Grandori, & Ilmoniemi, 1999; Szecsi, Götz, Pöllmann, & Straube, 2010; Ueno, et al., 1988a). Importantly, despite the diversity of available stimulation coils, all coils—including coils that aim at deeper stimulation—induce a stronger electric field on the cortical surface than in deeper locations (Heller & van Hulsteyn, 1992). Furthermore, there is a general trade-off between focality and depths of stimulation so that focal stimulation implies a rather shallow field, whereas coils with deeper spread of the field are nonfocal (Deng, et al., 2013; Deng, Lisanby, & Peterchev, 2014). Mathematical optimization that included coil arrays by way of mathematical design of the solution space identified the Pareto front, which confirms this depth–focality trade-off, although the optimal trade-off curve has yet to be achieved with presently available coils (Gomez, Cajko, Hernandez-Garcia, Grbic, & Michielssen, 2013). Advances in high-power metamaterial research could enable more optimal coil design in the future.

Early magnetic stimulation coils were mostly circular (Barker, et al., 1985; Polson, et al., 1982). Some had modifications such as an angulated extension in the otherwise circular winding, which turned out to have limited impact on focality (Cohen et al., 1990). Figure-of-eight coils consist of two loops each with several wire turns that meet in the center to form a strong focus underneath (Fig. 1B, 2A–C) (Ueno, et al., 1988a). There are several strategies for increasing stimulation focality. The eccentric figure-of-eight coil has higher density of winding turns toward the center of the coil where the two loops meet (Fig. 2D, 4C); this coil has better focality compared to the conventional figure-of-eight coil with the same outer dimensions (Knäulein & Weyh, 1996). Coils with more than two loops, such as in the cloverleaf coil (Fig. 2E), were proposed and used for peripheral nerve stimulation, but did not gain popularity (Roth et al., 1994; Ruohonen, Ravazzani, & Grandori, 1998).

There has been tremendous interest in building small TMS coils for animal studies and *in-vitro* experiments (and exploration of multichannel systems, see Section 3.1.4). The fundamental challenge is that diminishing head sizes reduce coupling to the TMS coil (Weissman, Epstein, & Davey, 1992), thus prohibitively high coil currents are required to achieve suprathreshold stimulation. Although small circular current components, e.g., generated by small coil loops, would allow strong foci and high-definition control over spatial field distributions, their implementation is associated with difficulties. First, due to the spatial low-pass filtering behavior of distance, strong foci generated by small current loops attenuate rapidly with distance and do often hardly reach the cortex. Second, pulse sources require a certain minimum inductance of stimulation coils, whereas the inductance of presented micro-coils is typically small, and the available space is small to increase the number of turns and ensure necessary high-voltage insulation in between. Third, the required current for an approximately constant induced electric field strength grows approximately inversely to the squared diameter of a loop. Thus, for a micro-coil with only one fifth of the diameter of a loop of a conventional figure-of-eight coil, the necessary current increases about 25-fold, leading to a current in the multi-digit kilo-ampere range. At the same time, the space for a conductor with sufficient cross section to sustain such high currents without damage is rarely available. At present, micro coils, such as ones used in some rodent or *in-vitro* studies (Tang, Makowiecki, Bartlett, & Rodger, 2015), can only produce subthreshold field strengths that fall into the so-called low field magnetic stimulation realm, which can have different physiological effects and mechanisms from conventional suprathreshold TMS.

For concurrent TMS and functional magnetic resonance imaging (MRI), appropriate MRI-compatible stimulation coils and positioning systems have been developed (Bestmann, Baudewig, Siebner, Rothwell, & Frahm, 2005; Bohning et al., 1999; Moisa, Pohmann, Ewald, & Thielscher, 2009). For MRI compatibility, coils primarily have to withstand the additional forces caused by the Lorentz-type interaction of the strong coil currents with the external field of the MRI scanner and a preferably symmetric field, e.g., as in planar figure-of-eight coils, to avoid the generation of rotational momentum. Furthermore, to avoid conventional squirrel-cage-like MRI head detection coils, Navarro de Lara et al. presented a flat head MRI head coil that can be inserted between the stimulation coil and the head (Navarro de Lara et al., 2015; Navarro de Lara et al., 2013).

3.1.2 Use of ferromagnetic material—Although the use of magnetically active materials for the guidance of magnetic fields, such as iron, is state of the art in electrical engineering, e.g., for transformers, the majority of magnetic stimulation coils are air coils (Volz, et al.). Magnetic materials with high permeability can guide and concentrate magnetic fields with low resistance to reduce the stray field outside the intended target as was demonstrated during the early days of TMS (Lorenzen & Weyh, 1992). Well known examples for such materials are ferromagnetic iron, cobalt, nickel as well as a number of compounds, ferrimagnetics (also known as ferrites), and rarely antiferromagnetics (Jiles, 2016). Academic devices as well as commercial systems showed that the appropriate use of magnetic core material allows more flexible shaping of the magnetic field as well as a reduction of the required pulse current in the coil to achieve the same field as air coils (Al-Mutawaly & Findlay, 1998; Davey & Epstein, 2000; Davey & Riehl, 2005; Deng, et al., 2008; Epstein & Davey, 1994; Epstein & Davey, 2002; Lorenzen & Weyh, 1992; Salvador, Miranda, Roth, & Zangen, 2007). Most designs use a C-shaped core (Fig. 3A, Figs. 4A and 4B), which was derived from a ring transformer with an air gap (Davey & Riehl, 2005; Epstein & Davey, 1994; Lorenzen & Weyh, 1992; Riehl, 2004; Riehl & Ghiron, 2005). Nevertheless, magnetic flux guidance with magnetic materials was also described to reduce the magnetic stray flux of designs known from air coils, such as circular and figure-of-eight coils (Barker, 2001; Ghiron, Riehl, & Shipway, 2014; Kim, Loukaides, Sykulski, & Georghious, 2004). For instance, ferromagnetic or ferrimagnetic material on the back of a figure-of-eight coil concentrates the necessarily closed magnetic flux lines on the back closer to the conductors so that the field energy is smaller for the same or even larger field strength in the target area (Fig. 2B and 3B). Ideally, such a steel backplane can shunt up to half of the field to reduce the energy content of the stray flux.

However, the conditions of magnetic stimulation risk substantial magnetic loss in magnetic-core coils and require a careful design. The high frequency components of the TMS coil current of 1 kHz – 10 kHz are orders of magnitude higher than the typical frequencies of 50 Hz and 60 Hz in power engineering as well as ~500 Hz in electric vehicles. The high fundamental frequency of TMS can lead to substantial loss in the magnetic material in the form of eddy currents, static hysteresis, and anomalous loss. Importantly, the eddy current loss grows notably stronger with both frequency f and the magnetic flux density B than the other loss contributions and is approximately proportional to the squared frequency, f^2, as well as the squared magnetic flux density, B^2 (Krings & Soulard, 2010).

The material selection of iron cores involves at least three degrees of freedom. Due to the high magnetic flux densities of TMS (~2 T), the material should show a high magnetic saturation level. For flux densities above the magnetic saturation, the differential magnetic permeability falls from initially greater than 100 down to 1, i.e., the permeability of air. If pulses exceed that magnetic saturation level, the electric AC resistance drops by more than one order of magnitude, causing a sharp rise of the coil current and potentially undesirably loading the stimulator circuit. To avoid large eddy-current losses and associated heating due to the high fundamental frequency of TMS pulse currents, the electrical conductivity of the material should be small. Strong field amplification in the target demands a high magnetic permeability. Ferromagnetic materials such as iron or silicon steel provide both high

saturation levels of up to approximately 2 T and high relative magnetic permeability of more than μ_r = 20,000, which both can be further improved by adding cobalt to the alloy, but are electrically conductive and require lamination to reduce eddy-current loss (Haiji, Okada, Hiratani, Abe, & Ninomiya, 1996; Littmann, 1967; Lorenzen & Weyh, 1992; Schmid, Weyh, & Meyer, 1993; Takada, Abe, Masuda, & Inagaki, 1988). Ferrites, on the other hand, are not electrically conductive and therefore present low loss, but saturate already at approximately 500 mT and offer lower relative permeabilities of ~1,000 (Gutfleisch et al., 2011; Ott, Wrba, & Lucke, 2003). Soft magnetic compounds (SMC), which contain small grains of soft-magnetic material in a nonconductive polymer matrix, may act as a compromise, but a use as a core material in magnetic stimulation coils has not been reported yet (Shokrollahi & Janghorban, 2007).

For the design and simulation process, various models for the nonlinear relationship of magnetic field strength H and the flux density B, which is also represented by the permeability μ, and magnetic loss in magnetic materials are known in the literature (Krings & Soulard, 2010). The Landau-Lifschitz equations as well as later modifications provide differential equations to describe the dynamics of domain-wall motion (Gilbert, 2004; Landau & Lifshitz, 1935). The Preisach, the Jiles-Atherton, and derived models describe B and H in relation of each other including hysteresis and can be incorporated into typical simulation systems used in TMS field modeling (Basso, Berlotti, Infortuna, & Pasquale, 1995; Bertotti, 1992; Bertotti, Basso, & Pasquale, 1994; Jiles & Atherton, 1986; Preisach, 1935). The simplest approach implements the nonlinearity as a look-up table and derives the magnetic loss in a post-processing step using the phenomenological approach by Bertotti et al. (Bertotti, 1988; Boglietti, Cavagnino, Lazzari, & Pastorelli, 2003).

3.1.3 Modified coil designs—Conventional coils induce electric fields with well-defined and temporally constant directionality. The local axes of the induced electric field at each location in the head stays the same throughout the entire duration of the pulse. The field of known coils thus has a fixed orientation relative to anatomic structures such as gyri and axons therein (Balslev, Braet, McAllister, & Miall, 2007). Rotem et al. presented a coil that rotates the induced electric field orientation during a pulse (Rotem et al., 2014). The demonstrated cloverleaf coil design is composed of two perpendicular figure-of-eight coils and requires two standard biphasic stimulators that are fired with a time delay that corresponds to a 90° phase shift of the underlying sinusoidal pulse. In experiments using conventional coils, neuronal activation is dependent on coil orientation; this directional sensitivity could be overcome with the rotating field coil design (D'Ostilio, et al., 2014; D'Ostilio, et al., 2016; Laakso, et al., 2014; Mills, et al., 1992; Rotem, et al., 2014).

The high loss of energy of a pulse of up to 100 J and the fast heating of stimulation coils has spurred work on superconducting coils. Superconducting stimulation coils would enable higher pulse amplitudes, faster pulse rhythms, and continuous long-term stimulation utilizing the latest protocols, such as theta burst (Friedman, Wolfus, Yeshurun, & Bar-Haim, 2004; Yang et al., 2010). However, the high currents of magnetic stimulation of up to 10 kA tend to be incompatible with the finite critical current densities of known superconductors (Lloberas, Sumper, Sanmarti, & Granados, 2014; Maeda & Yanagisawa, 2014). Above a few hundred Amperes per millimeter squared for the type-II high-temperature superconductor

YBaCuO, depending on the cryogenic operating temperature and material properties such as grain structure, the current's magnetic field influences the spin coupling of Cooper pairs—the essential charge carriers behind superconductivity—and renders superconductivity energetically unstable (Blatter, Feigel'man, Geshkenbein, Larkin, & Vinokur, 1994; Bugoslavsky et al., 2001; Palstra, Batlogg, van Dover, Schneemeyer, & Waszczak, 1989; Senoussi, 1992; Tixador et al., 2001). The effective cross section is further reduced due to screening currents that arise with the rapid alternating magnetic field during a pulse flow into the opposite direction of the intended coil current. These screening currents are also responsible for the diamagnetic behavior of superconductors, known as the Meissner effect (Larbalestier, Gurevich, Feldmann, & Polyanskii, 2001; Uglietti, Yanagisawa, Maeda, & Kiyoshi, 2010). Filamentation and Roebel structures, similar to Litz wires in conventional coils, can reduce such issues (Badcock et al., 2009; Hussennether, Oomen, Leghissa, & Neumüller, 2004; Long et al., 2008). Furthermore, most high-temperature superconductors are brittle and do not withstand the mechanical stress caused by the magnetic forces during a pulse without proper stabilization (Lloberas, et al., 2014). Due to further practicality issues in manufacturing and as the cooling effort is high and has to be implemented without substantially increasing the distance to the target, no successful superconducting TMS coil is known to date.

The high current surges during a pulse cause substantial mechanical forces in the pulse source, the cable, and the coil (Counter & Borg, 1992). These forces emit a loud clicking sound, which reaches the ears in two ways: through the air as well as bone conduction (Stenfelt & Goode, 2005). Due to its brevity, the clicking sound is typically underestimated with respect to its sound pressure level (Counter & Borg, 1992; Goetz et al., 2015; Starck, Rimpiläinen, Pyykkö, & Esko, 1996). There are reports of several cases of at least temporary hearing threshold shift and at least one case of permanent hearing loss associated with TMS in the literature (Counter, Borg, & Lofqvist, 1991; Loo et al., 2001; Pascual-Leone et al., 1993; Zangen, Roth, Voller, & Hallett, 2005). Even with earplugs for protection, the clicking sound distracts subjects and complicates the application of TMS during sleep. More importantly, despite earplugs, the TMS clicking sound activates auditory brain networks, which can dominate the intended TMS-induced brain activation (Bestmann, et al., 2005; Counter, 1994; Nikouline, Ruohonen, & Ilmoniemi, 1999; Siebner et al., 1999; Stenfelt & Goode, 2005; Tringali, Perrot, Collet, & Moulin, 2012). Modern coils use a stiff, rigid structure but could reduce the sound pressure only to a small amount. Vacuum casing as well as the use of shear coolants were proposed (Ghiron & Riehl, 2005; Ilmoniemi, Ruohonen, Kamppuri, & Virtanen, 1997). A recent solution implemented a coil structure with dedicated layers for acoustic decoupling and dissipation as well as pulses with its spectral content exclusively in the ultrasound range (Goetz, Murphy, & Peterchev, 2014; Peterchev, Murphy, & Goetz, 2015). For ultrasound, the sound impedances and absorption rates of most materials increase, the ear is less sensitive from a mechanical perspective, and safety levels are far higher (Howard, Hansen, & Zander, 2005; Möser & Kropp, 2010). In a demonstrator, the two-pronged approach reduced the sound pressure by more than 25 dB and the perceived psychoacoustic loudness of the coil click by 14-fold.

3.1.4. Inverse problem of optimum coils—Most coil simulation models analyze typically predefined coils and compared their performance (Deng, et al., 2013). Few analyses have been aimed at optimizing coil parameters such as winding thickness, radii, and other spatial characteristics in an analytical sense (Beyzavi & Nguyen, 2008; Jarmo Ruohonen, Virtanen, & Ilmoniemi, 1997). Recently, the computational TMS community increased its focus on numerical optimization of coils for specific objectives (Ilmoniemi, Koponen, Nieminen, & Järnefelt, 2013; Koponen, Nieminen, & Ilmoniemi, 2015; Starzynski, Szmurlo, & Sawicki, 2009). Most approaches embed physical electric field simulation models into iterative global optimization methods, such as genetic algorithms. Both realistic head models, e.g., solved with the finite element method, and idealized spherical models that allow accelerated semi-analytical solutions, such as spherical harmonics, can serve on the physics side (Gomez, et al., 2013; Starzynski, et al., 2009). A number of models parametrize coils, e.g., by radius, height, position, and overlap as well as cross section of individual coil components to maximize stimulation in a particular target (Starzynski, et al., 2009; Xu, Wang, Chen, Yang, & Yan, 2005). Alternative methods perform a widely unconstrained optimization without defining a certain parametric coil shape, but generate the extracranial current distribution required for the specific objectives almost freely (Gomez, et al., 2013; Ho et al., 2009; Koponen, et al., 2015). Koponen et al., for instance, decompose the field into basic components with increasing spatial frequency and varies the weights of each component in the superposed solution, i.e., the individual current, until the minimum energy objective is best met (Koponen, et al., 2015). The set of spatial components should span a more or less complete vector space and can use purely mathematical concepts such as Lissajous or Rose winding curves, discrete cosine modes as known from the JPEG image format, or Laplacian spherical harmonics for the current distribution. Alternatively, a multilayer coil can be constructed using a sequence of standard coils (e.g. Fig. 2F, layer 1: cloverleaf coil, layer 2: cloverleaf coil with a 45° rotation, layer 3: circular coil, layer 4: figure-of-eight coil in x-direction, layer 5: figure-of-eight coil in y-direction) (Ilmoniemi, Koponen, Nieminen, & Järneflt, 2014).

In the TMS community, numerical coil optimization seems to go hand-in-hand with another trend to design multi-focal or multi-channel micro-scale stimulation coils (Ho, et al., 2009; Laudani, Fulginei, & Salvini, 2015; Roth, Levkovitz, Pell, Ankry, & Zangen, 2014; Ruohonen & Ilmoniemi, 1998; Ruohonen, et al., 1999; Xiong, Shi, Hu, & Liu, 2016). Several approaches use a flat or curved grid of approximately equally sized loops (Han, Chun, Lee, & Lee, 2004; Ho, et al., 2009; Laudani, et al., 2015; Ruohonen & Ilmoniemi, 1998; Ruohonen, et al., 1999; X. Wang, Chen, Guo, & Wang, 2005). Alternatively, Ge et al. use a grid of vertical and horizontal lines mapped onto a head instead of loops (Ge, Wang, Tang, Xiao, & Wu, 2012). A ring current can be generated by controlling the current of two vertical and two horizontal lines appropriately. As such, the grid structure resembles address lines in TFT screens or historic computer memory. Optimization in such framework adjusts the current amplitude in the individual loops or the conductors of a linear grid to optimize certain objectives, such as the electric field in a predefined target while minimizing the overall field energy or co-activation elsewhere (Gomez, et al., 2013). Indeed, if the current share of each channel is fixed and not used to dynamically change between several neural targets, the currents of the individual channels of the multichannel coils can be

mathematically converted into an overall planar current distribution and be approximated with an equivalent winding pattern that does not contain the regular grid of loops any more. However, many multichannel coil approaches are widely naïve to manufacturing coils and to the necessary high currents in the kilo-ampere range, which increase inversely to the square of the coil size. Other implementation challenges include: coupling between the channels that may distort the stimulator circuit operation; the heating and forces associated with small coil elements; and complex electronic control of independent channel currents. Accordingly, most articles on multichannel TMS still lack reports on a successful implementation and experimental data.

3.2 Stimulators and waveforms

Whereas the stimulation coil determines the spatial field conditions, the stimulator or pulse source generates the pulse current and is responsible for the temporal aspects (see Fig. 5) (Jalinous, 1991). Because the electrical parameters of commercial systems have converged to very similar values, pulse sources are typically general-purpose devices that can feed a variety of coils. The challenge for pulse sources is the combination of very high currents and the briefness of stimulation pulses, which exceed the range of conventional electronics technologies such as amplifiers. Most pulse sources therefore exclusively use an electrical oscillator design with a pre-charged capacitor and a power switch in the device and an inductance represented by the stimulation coil to form a more or less damped sinusoidal current shape (Peterchev, et al., 2015; Polson, et al., 1982). Closing the switch establishes a current oscillation between the pre-charged capacitor and the stimulation coil, which can: be damped with a resistor to slowly return to zero and form so-called monophasic pulses (Fig. 6A); be terminated after one period to generate so-called biphasic pulses; or left oscillating for several periods to form polyphasic pulses (Fig. 6B) (Peterchev, et al., 2015). However, the oscillator that is formed by closing the switch depends on the components only and cannot be changed without reconfiguring the circuit. Several devices that could generate pulses different to these standard pulses, such as sinusoidal half-wave pulses with up to 400 μs duration as well as rectangular and trapezoidal pulses, were presented, but none of these could adjust the pulse shape over a wider range during operation (Havel et al., 1997; J. F. Nielsen, Klemar, & Kiilerich, 1995). The prevailing switch in TMS devices is the thyristor, a type of controllable electrical diode that can only be turned on but not actively turned off. From the time of triggering the pulse on, the circuit is no longer controlled from outside. In consequence, the pulses of most available TMS stimulators are fixed with respect to pulse duration and shape. Practical aspects for device implementation of prevailing conventional devices are discussed in detail in the literature (Al-Mutawaly & de Bruin, 2001; Cadwell, 1991; Jalinous, 1991; McRobbie, 1985; Wolf & Walker, 1991).

Recent developments have achieved overcoming the pulse-shape limitation and allow adjusting the shape during operation. Several refinements of a TMS technology that enables the configuration of pulse parameters (cTMS) have been demonstrated and are available commercially (Fig. 6C) (Peterchev, D'Ostilio, Rothwell, & Murphy, 2014; Peterchev, Jalinous, & Lisanby, 2008; Peterchev, et al., 2011). cTMS splits a pulse into few near-rectangular voltage segments, which can be adjusted in amplitude and duration. Modern high-voltage high-power semiconductor devices—specifically insulated gate bipolar

transistors (IGBT)—let cTMS actively commutate the coil current between two capacitors with different capacitance and arbitrary initial charge level. A pulse can be assembled of phase segments selecting from three different electric field amplitude levels, while the three amplitude levels can be slightly changed between consecutive pulses in a train (Peterchev, D'Ostilio, Rothwell, & Murphy, 2014).

More flexibility and increased control over the pulse shape as well as the combination of pulses in a train require giving up a number of conventions of TMS electronics, including slow high-power switches and the oscillator design. A recently developed modular pulse synthesizer technology, for instance, does not implement an oscillator design but combines the output of multiple fast-switching lower power modules to generate practically any pulse shape as well as trains of rapidly changing pulse shapes (Fig. 6D) (Goetz et al., 2016; Goetz, Peterchev, & Weyh, 2015; Goetz, Pfaeffl, et al., 2012). In contrast to, for instance, conventional monophasic pulse sources, the principle of the modular pulse synthesizer is highly efficient and can recover most of the energy of any pulse shape for the next pulse. Thus, it can also generate the monophasic pulse shape at high repetition rates.

4 Models of the induced electric field distribution

4.1 Modeling approaches and technical aspects

The key phenomenon behind magnetic stimulation is electromagnetic induction. Mathematically, the induced electric field is derived through differential operators that act spatially and temporally on the magnetic field. In the operating frequencies of TMS (< 10 kHz), the quasi-static approximation allows that the spatial distribution of the magnetic field can be decoupled from its temporal dynamics (Bossetti, Birdno, & Grill, 2008). Numerically, the calculation of induced currents tends to instability as is known from other disciplines (Beck, Hiptmair, & Wohlmuth, 1999; Biro & Preis, 1990; Biro, Preis, Buchgraber, & Ticar, 2004; Clemens, Wilke, & Weiland, 2001; Hollaus & Biro, 2000; Soleimani, Lionheart, Peyton, Xiandong, & Higson, 2006; Wong & Cendes, 1989). In magnetic stimulation, stability is further complicated by the nonideal geometry in case of realistic models and because the coil currents and the induced currents in the brain differ by at least six orders of magnitude but are numerically tightly coupled in Maxwell's equations as well as the double-curl equation that is derived from them using the Helmholtz decomposition. To enhance stability and increase speed, magnetic stimulation has been modeled with a variety of equation systems derived from Maxwell's equations. Alternative equation systems are, for instance, the T-Ω formulation to enforce stability by a more appropriate choice of potentials, and various ways to decouple the coil and the induced currents so that the back-action of the small induced current on the coil current (Goetz, Afinowi, et al., 2013; Golestanirad, Mattes, Mosig, & Pollo, 2010; Miranda, Hallett, & Basser, 2003; Opitz, et al., 2011; Sawicki, Starzynski, & Wincenciak, 2006; Thielscher, Opitz, & Windhoff, 2011; Wagner et al., 2008; Wagner et al., 2014; Yang et al., 2006). The so-called A-V formulation of the magnetic field first solves the magnetic vector potential (A), then in a second step, derives the electric scalar potential (V). For the computational solution of these partial differential equations, researchers in the field use several different approaches, including finite difference methods (Fanjul-Vélez, Salas-García, Ortega-

Quijano, & Arce-Diego, 2015; Toschi, Welt, Guerrisi, & Keck, 2008, 2009), finite volume methods (Goetz, Afinowi, et al., 2013; He & Liu, 2016), boundary element methods (Im & Lee, 2006; Nummenmaa et al., 2013; Salinas, Lancaster, & Fox, 2009), and impedance methods (De Geeter, Crevecoeur, & Dupre, 2011; De Geeter, Crevecoeur, Dupré, Van Hecke, & Leemans, 2012; De Geeter, Crevecoeur, Leemans, & Dupré, 2015; Nadeem, Thorlin, Gandhi, & Persson, 2003), while finite element methods (FEM) dominate (Bijsterbosch, Barker, Lee, & Woodruff, 2012; Chen & Mogul, 2009; Deng, et al., 2013; Janssen et al., 2013; Laakso & Hirata, 2012; Laakso, et al., 2014; W. H. Lee, Lisanby, Laine, & Peterchev, 2014; Miranda, et al., 2003; Opitz, et al., 2011; Masaki Sekino & Ueno, 2002; Thielscher, et al., 2011; Windhoff, Opitz, & Thielscher, 2013).

4.2 Simplified models

The early three-dimensional spatial models of magnetic stimulation were generally based on simplified and symmetric geometry, such as infinite half-planes and perfect spheres. For example, in a magnetic coil design study, the brain was approximated using a quasi-spherical volume conductor, enclosed by 58 planes (Ueno, Tashiro, & Harada, 1988b). In the theoretical model proposed by Rush and Driscoll (Rush & Driscoll, 1968), the head was modeled as three conducting concentric spherical shells consisting of the scalp, skull, and brain tissue. Each shell is considered as homogeneous with a dielectric property of the tissue it represents (Al-Mutawaly & Findlay, 1998; Deng, et al., 2013; Deng, Lisanby, & Peterchev, 2015; Deng, et al., 2008; Miranda, Lomarev, & Hallett, 2006; Ravazzani, Ruohonen, Grandori, & Tognola, 1996). With increasing computational power, progress in brain imaging, and available software tools, spherical head models were replaced by still idealized imaging-based head models (Fig. 8A) (Masaki Sekino & Ueno, 2002; Sekino & Ueno, 2004; Wagner, et al., 2008; Wagner, et al., 2004; Yang, et al., 2006) and finally gyri-precise realistic head models (Fig. 8B) (Cerri, De Leo, Moglie, & Schiavoni, 1995; Chen & Mogul, 2009; Im & Lee, 2006; Nadeem, et al., 2003; Salinas, et al., 2009). While spherical head models predict the absence of radial currents induced by TMS, which falsely justified the claim that only interneurons tangential to the cortical surface are stimulated during TMS, realistic head models showed otherwise. There were also gross discrepancies between spherical and realistic head models, and the differences are more pronounced for temporal and frontal targets (Nummenmaa, et al., 2013). Nevertheless, spherical models have been useful for TMS coil design (Davey & Riehl, 2006; Deng, Peterchev, & Lisanby, 2008; Ruohonen & Ilmoniemi, 1998) and evaluation of stimulation sites (Thielscher & Kammer, 2002).

As a consequence of the macroscopic treatment of the problem, the representation of the head as an assembly of different materials forms abrupt material interfaces, e.g., between white and grey matter, where electrical parameters such as the conductivity can change by a factor of two (Bijsterbosch, et al., 2012). In simulation models, this abrupt step in conductivity leads to charge accumulation and therefore strong local electric fields at the interface (Kent Davey, Epstein, George, & Bohning, 2003; Silva, Basser, & Miranda, 2008). However, the brain microanatomy does not show such abrupt changes but is notably less defined and fringed. Furthermore, the currently prevailing model of neural activation by TMS considers the intra-axonal electric field responsible for neural activation, which is only

peripherally affected by such extra-axonal interfaces (Roth & Basser, 1990). The interaction between macroscopic field modeling and the axonal membrane is not based on a consistent theory and may require more research in the future.

4.3 Models with increased level of detail

One way to increase the accuracy of the tissue-property representation introduces anisotropy, particularly of the electric conductivity. Due to the fibrous structure, white matter shows a by up to one order of magnitude higher conductivity along the dominant fiber orientation (Gabriel, Peyman, & Grant, 2009). Models implementing anisotropy extract the local fiber orientation from diffusion tensor imaging (DTI) and show minor changes for the electric field in the grey matter and the position of the stimulation focus, but local electric field amplitudes differ by up to approximately 20% (Fig. 8C and 8D) (De Geeter, et al., 2012; De Geeter, et al., 2015; De Lucia, Parker, Embleton, Newton, & Walsh, 2007; Lee et al., 2012; Lee, Lisanby, Laine, & Peterchev, 2016; Miranda, et al., 2003). Nummenmaa et al. further used DTI data to extract the local fiber orientation at the gyral crown in the focus to determine the optimal coil position for stimulation (Nummenmaa et al., 2014).

Due to cerebrospinal fluid (CSF) having a higher conductivity by a factor of approximately 5 to 20 times compared to other brain tissue, the exact location and the interface with the grey matter has a dominant influence on the field strengths in the grey matter and exceeds the influence of the interface between the grey and the white matter (Bijsterbosch, et al., 2012; Janssen, et al., 2013; Miranda, et al., 2003; Wagner, et al., 2008). Realistic head models found that the increase of the electric field in the gyral crowns is far beyond what the lower distance of these areas to the stimulation coil would explain (Bijsterbosch, et al., 2012). The highest electric fields in the brain emerge where the CSF is thinnest (Bijsterbosch, et al., 2012; Janssen, et al., 2013). With respect to modeling quality, an accurate segmentation of the surface between CSF and grey matter and a realistic representation of local thicknesses of the CSF layer therefore seems highly important. Both can suffer in automatic segmentation, which is known to show limited reliability particularly at these interfaces (de Boer et al., 2010; Eggert, Sommer, Jansen, Kircher, & Konrad, 2012; Klauschen, Goldman, Barra, Meyer-Lindenberg, & Lundervold, 2009). Janssen et al. studied the influence of a misestimated surface of the grey matter by eroding as well as growing the gyrus systematically starting from a reference segmentation and wound changes of electric field strength particularly in the surface of the grey matter and the vicinity (Janssen, et al., 2013). Importantly, CSF also affects focality. The more pronounced the sulci between gyri are modeled the wider the focus becomes spread over one or several gyri (see Fig. 8) (Janssen, Oostendorp, & Stegeman, 2015; Janssen, et al., 2013). Furthermore, CSF and its modeling can notably shift the actual focus of stimulation determined by the electric field magnitude vs. the assumed focus given by the coil axis (Bijsterbosch, et al., 2012). Several sensitivity analyses derived statistical information in which way important parameters, e.g., tissue conductivity, coil position and orientation, as well as uncertainties in such parameters influence the focus and the effective stimulation strength in the target (Gomez, Yücel, Hernandez-Garcia, Taylor, & Michielssen, 2015; Toschi, Keck, Welt, & Guerrisi, 2012). Such parameter sensitivity analyses typically use Monte-Carlo methods or models that do not process physical metrics but statistics, i.e., distributional information thereof.

Modern personal computers have reached sufficient computational power that the induced electric field can be estimated in real time. Consequently, highly simplified spatial field models can be introduced into frameless stereotactic neuronavigation systems, where they are overlaid with the brain anatomy (Comeau, 2014; Nummenmaa, et al., 2013; Ruohonen & Karhu, 2010). As realistic head models easily overwhelm computers, spherical head models with homogeneous tissue properties, i.e., one bulk conductivity, scaled to the specific head dimensions prevail. However, targeting with neuronavigation is usually performed on the gyral and sub-gyral level so that the missing anatomic fine structure and effects such as spreading of the focus across gyri could mislead (Sahlsten et al., 2015). A realistic model framework with substantially reduced spatial resolution of 3 mm that applies the admittance method and eliminates the back-action of the brain fields on the coil current was proposed to bring computation times to the order of ~20 s (Paffi et al., 2015). Fast parallel computation on graphics processors and Green's function approaches may allow the use of more realistic anatomy in the future.

At present, electric field models in magnetic stimulation typically neglect the cellular structure of biological tissue as well as membranes but treat the brain as an assembly of homogeneous compartments of materials with average properties, such as electrical conductivity and permittivity. The electrical conductivity macroscopically describes the effective mobility of electric charge carriers through the cellular tissue (Gabriel, et al., 2009). A large permittivity results from the high number of thin cell membranes, which act as capacitors, and causes displacement currents. Whereas many TMS field simulation models neglect the permittivity (Bijsterbosch, et al., 2012; Goodwin & Butson, 2015; Janssen, et al., 2013), De Geeter et al. identified the permittivity to be responsible for about 20% of the field strength in the focus of the coil (De Geeter, et al., 2012). Furthermore, permittivity values used in TMS models are based on *ex-vivo* measurements, where membranes may have degraded, and have been suspected to underestimate *in-vivo* conditions (Gabriel, Lau, & Gabriel, 1996; Wagner, et al., 2014).

Finally, stimulation coils are often still represented by idealized geometries, such as single or double tori or hollow cylinders with only one loop in which the current either freely distributes in the simulation or with enforced constant current density (see Fig. 7). For an accurate estimation of the electric field distribution in the target, however, precise coil models need to incorporate the individual turns of a coil to account for proximity and skin effects, which can reduce the simulation error by up to 30% (Laakso & Hirata, 2012; Laakso, et al., 2014; Nadeem, et al., 2003; Salinas, et al., 2009).

5 Models of the neural activation process

5.1 Phenomenological neuron models

Neuron models fill the deficiency that above-described spatial models can only describe the field distribution but do not include the actual neural response. A number of neuron models with different levels of detail are in use for simulating the neural response to TMS. These models include purely mathematical descriptions that mimic neural behavior as well as models reflecting the actual biological and physical mechanisms on the level of the neural membrane.

The simplest model in TMS research is the leaky integrate-and-fire neuron (Bostock, 1983; Corthout, et al., 2001; Lapicque, 1907; Peterchev, et al., 2011). This model describes the excitable neural membrane as a leaking electrical capacitor, i.e., a parallel connection of a capacitor C, which can be charged up by stimulation, and a resistor R, which discharges the capacitor with a time-constant of $\tau = RC$. Some of these first-order models have a built-in resetting property, that is, when the depolarization exceeds a predefined threshold level, the model spikes and is reset to zero (Brunel & van Rossum, 2007; Izhikevich, 2004). By itself, the leaky integrate-and-fire neuron model is a low-pass filter with respect to the stimulator output amplitude and reflects the well-known strength-duration curve (Corthout, et al., 2001). Due to its low number of parameters, the leaky integrate-and-fire model can be noninvasively calibrated to real neurons *in-vivo* (Corthout, et al., 2001; D'Ostilio, et al., 2016; Peterchev, et al., 2013) (Deng, Lisanby, & Peterchev, 2011). The use of different coil orientations was reported to enable such system identification for specific neuron populations in the same cortical target volume (D'Ostilio, et al., 2014; D'Ostilio, et al., 2016). The leaky integrate-and-fire model may be sufficient for predicting trends and if the tested pulse shapes belong to the same class, i.e., that the pulses are typically related to each other by expansion and compression. However, as a highly simplified passive model with exclusively linear dynamics, it does not reflect the complex nonlinear active mechanisms of neurons. It is known to show deviations, e.g., when the pulse shape is substantially varied, for short pulses, and for double pulses as well as polyphasic pulses (Fang & Mortimer, 1991; Maccabee et al., 1998; Moffitt, McIntyre, & Grill, 2004). These deviations are also known in electrical stimulation (Bennie, Petrofsky, Nisperos, Tsurudome, & Laymon, 2002; Buetikofer & Lawrence, 1978, 1979; Dean & Lawrence, 1985; Gorman & Mortimer, 1983; Grill & Mortimer, 1995; A. Wongsarnpigoon, Woock, & Grill, 2010).

5.2 Biophysical neuron models

More accurate nonlinear neuron models include several purely mathematical representations without further biophysical meaning such as the FitzHugh-Nagumo, the Hindmarsh-Rose, and the Izhikevich models (d'Aloja, Lino, Maione, & Rizzo, 2005; d'Aloja, Lino, Maione, & Rizzo, 2007; FitzHugh, 1961; Hindmarsh & Rose, 1984; Izhikevich, 2003; Nagumo, Arimoto, & Yoshizawa, 1962; Suárez-Bagnasco, Armentano-Feijoo, & Suárez-Ántola, 2010; Xiu Wang, Wang, Deng, Wei, & Li, 2013). However, due to the high numbers of parameters of these models despite the limited mechanistic insight, biophysical models dominate at present. Biophysical models used in the TMS community typically follow the formalism of Hodgkin and Huxley, who described the neuron activation dynamics in electrical circuit models with nonlinear elements representing different ion conduction mechanisms, which were later discovered as ion channels (Hodgkin & Huxley, 1952). The Hodgkin-Huxley model describes the giant squid axon, which notably deviates from mammalian and particularly human neurons. The expansion of the formalism of equivalent electric circuits to add spatial characteristics of neurons initiated modern one-dimensional compartment models (McNeal, 1976; Scott, 1975). The concept of equivalent electrical circuits has been substantially expanded in computational neuroscience and led, for instance, to complex circuit models of entire motor units or for computational simulation of neuromodulation (Peasgood, Dissado, Lam, Armstrong, & Wood, 2003; Szlavik, 2008; Szlavik, Bhuiyan, Carver, & Jenkins, 2006; Szlavik & de Bruin, 1999).

Latest neuron models using the same formalism though different parameters are available for various mammalian neuron parts such as axon, soma, and dendrites as well as for their subsegments such as the axon initial segment, myelinated axon sections, and axonal nodes as these are known to differ with respect to expressed ion channel types and their densities on the membrane surface (Baker, Bostock, Grafe, & Martius, 1987; Bender & Trussell, 2012; Kole et al., 2008; McIntyre, Richardson, & Grill, 2002; Scholz, Reid, Vogel, & Bostock, 1993; Schwarz, Reid, & Bostock, 1995; Stephanova & Bostock, 1995). More complicated patterns of local accumulations that may affect excitability to TMS stimuli such as ion channel rafts have not been studied yet (Freeman, Desmazières, Fricker, Lubetzki, & Sol-Foulon, 2016; Kole & Stuart, 2012; Rasband & Peles, 2016; Vacher & Trimmer, 2012). In multi-compartment models, these segments and subsegments are combined to represent entire neurons (Kamitani, Bhalodia, Kubota, & Shimojo, 2001; McIntyre, et al., 2002; Salvador, Silva, Basser, & Miranda, 2011b).

Neuron models in TMS research have been set up as stand-alone models as well as implemented into spatial brain models. Stand-alone neuron models neglect the induction process as well as the spatial influence of the brain and can therefore not predict absolute thresholds without calibration but allow relative comparisons (Reilly, 1989). One important aspect of stand-alone neural models for TMS is the study of the neural activation process. A solid understanding of the neural activation process is, for instance, essential for the design of pulse shapes for effective activation of neurons (Corthout, et al., 2001).

5.3 Applications of neuron models

Important questions raised in the TMS community that could be solved by neuron models are the well-known experimental observations that biphasic pulses effectively stimulate, although they appear to compensate their depolarizing phase by their hyperpolarizing phase(s) and that polyphasic pulses even further decrease the threshold (Emrich, et al., 2012; Goetz, Weyh, & Herzog, 2009; Maccabee, et al., 1998; Pechmann et al., 2012). Similarly, neural models explain the higher threshold of monophasic relative to biphasic pulses as well as directional effects of the monophasic pulse shape (Salvador, et al., 2011b).

Head and single-neuron models well describe the spatial and temporal aspects of the initial activation process of single pulses. These models, however, cannot describe nor optimize neuromodulation effects. Neuromodulation phenomena as the basis of most cognitive research applications as well as therapeutic interventions of TMS emerge if several pulses are combined with certain timing constraints and trigger network effects. Esser et al. designed an appropriate large-scale thalamo-cortical model (Esser, Hill, & Tononi, 2005). The model includes > 30,000 neurons with > 5,000,000 synaptic connections in layers 2/3, 5, and 6 of the primary motor cortex and the thalamus with afferents from premotor and somatosensory circuits, but excludes spatial field calculations as well as activation dynamics, which were the center of above-described models. Each neuron is implemented as a simplified nonlinear single-compartment model with sodium and potassium channels to simulate physiological spiking behavior, though without the need for exact representation of the TMS activation process at the axonal membrane. Instead TMS pulses can be implemented by an activation of a predefined portion of synapses, while the portion

increases for higher pulse amplitudes (Esser, et al., 2005). The model mimics the phenomenon that individual TMS pulses of sufficient amplitude cause several cortico-spinal responses, so-called I waves (Di Lazzaro, et al., 2012; Di Lazzaro, Ziemann, & Lemon, 2008; Esser, et al., 2005). With increasing pulse amplitude, the first wave, I1, is followed by up to three subsequently emerging additional responses, I2, I3, and I4, each ~ 1.5 ms apart. The model hypothesizes the multiple I waves to emerge from layer 5, where the density of inhibitory cells is considered and modeled lower than in upper cortical layers (Beaulieu, 1993).

An alternative model for the generation of I waves by d'Aloja et al. was implemented with a network of 500 cortical neurons and 100 corticospinal neurons, each of them represented by an Izhikevich spiking unit (d'Aloja, et al., 2005). The cortical neurons form a highly interconnected network, and each corticospinal neuron receives inputs from five cortical neurons. Rusu et al., in contrast, aim at explaining the I-wave generation in a model of a single pyramidal cell (Rusu, Murakami, Ziemann, & Triesch, 2014). The authors hypothesize that all could result from signal delays due to synaptic distance from the soma. However, general knowledge gaps of the mechanisms behind neuromodulation affect the predictive quality of corresponding models. As a consequence, essential outcomes in Rusu et al., e.g., the delays, are set as a-priori parameters, so that the model is not clearly falsifiable from an epistemological perspective and therefore risk a model without predictive qualities (Popper, 2005). Esser et al. rely on weaker assumptions, such as an increasing portion of excitatory neurons from layer 2 to layer 5 (Esser, et al., 2005).

More detailed models were designed to further describe and explain neuromodulation on the synaptic level. Huang et al. implemented a calcium-concentration based model (Huang, Rothwell, Chen, Lu, & Chuang, 2011). The model assumed a mixed effect of slow inhibition and fast facilitation dynamics to explain theta-burst stimulation. Since the dynamics of the development of inhibition and facilitation differ in this model, it further provides a potential explanation for the train-length-dependent neuromodulation effect of theta-burst stimulation.

Neuron models in TMS not only serve as an analytic tool to study existing technology and pulse shapes. Models are increasingly used to synthesize both novel pulse shapes and more effective pulse trains (Goetz, Truong, et al., 2013; Goetz, Truong, et al., 2012; Wilson, Goodwin, Brownjohn, Shemmell, & Reynolds, 2014). At present, new pulse shapes were studied and improved particularly with respect to their physical parameters, such as the specific stimulation threshold, associated coil heating, and acoustics. Parameter studies of pulse shapes started to explore ranges of pulse shapes that are not implemented in commercial TMS devices. Recent approaches freely synthesize TMS pulse shapes to find global optima by solving the underlying variational problem (Goetz, Truong, et al., 2013; Goetz, Truong, et al., 2012). Similar approaches are in progress for transcutaneous and invasive electrical stimulation (Jezernik, Sinkjaer, & Morari, 2010; Wongsarnpigoon & Warren, 2010; Wongsarnpigoon, et al., 2010). For the improvement of neuromodulation protocols, on the other hand, Wilson et al. performed parameter sweeps for continuous trains and bursts with a wide range of burst rates and no. of pulses (Fung, Haber, & Robinson, 2013; Robinson, 2011; Wilson, et al., 2014).

5.4 Integration of neuron models into spatial models

For the prediction of absolute stimulation thresholds and coil orientation effects, neuron models are incorporated into realistic head models (Goodwin & Butson, 2015; Salvador, et al., 2011b). Typically, such studies solve the spatial field distribution stationary sinusoidal or transient realistic pulse shape and subsequently feed the local electric field properties into a one-dimensional neuron model. This approach generates a loose forward coupling between the spatial as well as the neuron model and simplifies the interaction of the neural membrane and its surrounding. Salvador et al., for instance, combine a realistic spatial sulcus model with a dozen dynamical neuron models (Salvador, Silva, Basser, & Miranda, 2011a). In the coupling step, the electric field are extracted from a finite-element software tool and transferred to the Neuron stimulation environment (Yale University, New Haven, CT) to calculate the axonal response. Despite limitations because of the highly-simplified interface at the membrane, Salvador et al. could demonstrate the experimentally well-known threshold difference between mono- and biphasic and the threshold reduction for posterior-anterior induced current direction (Salvador, et al., 2011b). Agudelo-Toro et al., in contrast, presented a notable spatial model that avoids these simplifications, which are widely used for coupling neurons to spatial models, and incorporates the microscopic neuron with all its spatial characteristics including the membrane into a finite-element model (Agudelo-Toro & Neef, 2013). The necessary equations for such an approach are long known (Scott, 1975). However, Agudelo-Toro and colleagues simplified the equation system to achieve computation times in an acceptable range of minutes to few hours.

6. Model-based experimental methods

Most computational models in TMS are autonomously set up based on fundamental physical and physiological relationships, while simple calibration of parameters may be taken from experiments. There is an increasing trend of combining models and experiments. The combination of both can improve theoretical mechanistic insight as well as prediction abilities, for instance, when models are calibrated and validated in a closed-loop setup that optimally picks stimuli such that it decreases the parameter estimation errors most efficiently (Alavi, Goetz, & Peterchev, 2016; Goetz, Whiting, & Peterchev, 2011; Treutwein & Strasburger, 1999). Furthermore, the combination can enhance experimental abilities by the extraction of otherwise inaccessible quantities or information and by revealing underlying interactions in the brain, which may serve as novel diagnostic tools for psychiatry and neurology.

A prominent target of combined experimental-modeling methods is neural recruitment in the motor system. Stimuli in the motor cortex are known to evoke corticospinal responses that travel along the spine to a peripheral muscle and activate a peripheral muscle, which can be detected electrically as a motor-evoked potential (MEP). The response amplitude and latency of the MEP wave depends on several extrinsic parameters such as stimulation strength, stimulus properties, as well as pulse dynamics; there is further a large number of intrinsic anatomical and physiological factors that can be extracted with appropriate model learning techniques (Peterchev, et al., 2013; Rösler, 2001). The input–output behavior, including the sigmoid recruitment that is on average formed by the MEP size as a function of stimulation

strength, is a sensitive marker for various pharmaceuticals as well as neurological disorders and a predictor for motor recovery (Boroojerdi, Battaglia, Muellbacher, & Cohen, 2001; Caramia et al., 1991; Carroll, Riek, & Carson, 2001; Julkunen, Ruohonen, Sääskilahti, Säisänen, & Karhu, 2011; Kaelin-Lang & Cohen, 2000; Malcolm et al., 2006; Pitcher, Ogston, & Miles, 2003; Thomas & Gorassini, 2005; van Kuijk et al., 2009; van Kuijk, Pasman, Hendricks, Zwarts, & Geurts, 2009).

An underestimated component in the input–output behavior is the trial-to-trial variability of MEPs, which can vary by orders of magnitude, although there are no differences of extrinsic conditions or coil movements (Brouwer & Qiao, 1995; Ellaway et al., 1998; Gugino et al., 2001; Rösler, Roth, & Magistris, 2008). This variability was observed to show an intricate statistical distribution, to change in the presence of various drugs and brain injuries, and to be to a large part a correlate of ongoing endogenous neuromodulation on the cortical and spinal level (Darling, Wolf, & Butler, 2006; Devanne, Lavoie, & Capaday, 1997; Kaelin-Lang et al., 2002; Mitchell, Baker, & Baker, 2007; Moosavi, Ellaway, Catley, Stokes, & Haque, 1999; Nielsen, 1996; Choudhury et al., 2011; Zarkowski, Shin, Dang, Russo, & Avery, 2006). Model-based decomposition techniques were developed with the aim to turn TMS into a tool to observe ongoing signaling in a neural circuit, similar to the detection of postsynaptic potentials with patch-clamp techniques. The underlying models of the corticospinal input–output system incorporate various sources of variability and are designed to be calibrated to a subject (Fig. 9) (Goetz, Luber, Lisanby, & Peterchev, 2014; Goetz & Peterchev, 2012). By the calibration, the overall variability is decomposed so that for each MEP the contribution of the various variability sources can be quantified to reconstruct the inhibitory or excitatory input to the stimulated neurons at the time of stimulation.

Similarly, the triple-stimulation method is based on a high-level neural model of the spinal and peripheral pathway from signals from the brain to the muscle (Magistris, Rösler, Truffert, & Myers, 1998). This method applies an electrical stimulus, e.g., at the wrist shortly after the TMS stimulus in the motor cortex to cancel out the original stimulus by its antidromic signal. A third peripheral stimulus is applied proximally to the cancellation point, which only successfully passes on along those fibers where the previous antidromic signals have cancelled out already. This method can estimate the number of activated motor units and detect the phase relationship of descending MEP and can isolate the trial-to-trial variability of MEPs that results from phase desynchronization. In diagnostics, the triple stimulation technique showed more than two-times higher sensitivity for neural dysfunction than the measurement of MEP amplitudes and latencies (Magistris, Rösler, Truffert, Landis, & Hess, 1999).

The approach to combine experiment and modeling to extract otherwise covert information has further been expanded to TMS with concurrent electroencephalography (EEG). Cona et al. developed a neural mass model for TMS-evoked potentials (TEP) (Cona, Zavaglia, Massimini, Rosanova, & Ursino, 2011; Ursino, Cona, & Zavaglia, 2010). The model includes cortical columns with four neuron populations—pyramidal neurons, excitatory glutamatergic interneurons, fast $GABA_A$ interneurons, and slow $GABA_A$ interneurons—from three cortical sites—the occipital, the parietal, and the frontal lobes, while the pyramidal neurons implement the interconnection of the sites. Cona et al. calibrated the

model to subjects to mimic the first 200 ms of TEPs with high correlation. The model predicts the TEP response including individual components at the site of stimulation as well as at the other sites to where it is relayed through projections. The calibrated model further reveals information about the connectivity of the used cortical areas as well as variability, both of which are not accessible directly (Cona, et al., 2011). However, these models do not currently distinguish different physiological sources of response to TMS, such as auditory and somatosensory contributions to the evoked potentials.

7. Conclusions

Computational modeling plays an important role throughout the entire field of magnetic stimulation for developing improved equipment and understanding how magnetic stimuli interact with the brain. Increasingly realistic and detailed models are unmatched in many aspects of TMS for uncovering mechanisms since the interaction of TMS with the brain is complex due to the high degree of positive and negative feedback as well as interference with endogenous brain activity. Since there is typically no access to internal processes, the response to TMS is hardly predictable or understandable without modeling. The importance of detailed models will further grow as experimental procedures increase in complexity, as devices give experimenters more control, e.g., over the pulse shape, and as easy-to-use simulation tools become available (Peterchev, et al., 2014; Windhoff, et al., 2013). For the foreseeable future, it appears likely that more and more experimenters will simulate their experiments to plan the procedure, analyze the outcome, and predict behavior.

However, modeling of TMS runs a serious risk that is often ignored, but harms scientific integrity. Due to the high complexity of neural interaction with TMS, inappropriate modeling easily becomes post-hoc and inductive. That occurs if models, particularly models with many parameters, are fit to an outcome, but are not able to predict more than the data they were fit to. To be scientifically sound, a model needs to always make predictions that go beyond the data used to set up the model—preferably predictions that the authors of the model cannot answer by the time the model is set up. Those predictions are the key to test, validate, potentially falsify the model or find limitations (Popper, 2005). Authors of models should therefore clearly report the data and observations used for model regression, assumptions their models were set up with, and how parameters were estimated and incorporated. Outcomes that are to be explained must not be implemented as parameters into the model. The risk for inductive modeling is further aggravated if models provide high complexity with multiple feedback loops and a large set of parameters. Furthermore, authors should be encouraged and always present testable predictions based on their models, which are clearly marked as such. The report of such predictions for validation is enforced in other disciplines that are particularly susceptible to nonobvious inductive models, such as statistics and machine learning (Babyak, 2004; Drummond & Japkowicz, 2010; Hawkins & Kraker, 2010; Langley, 1988). A number of models in the literature of magnetic stimulation thus far do not reach that quality level. Falsifiable and falsified models should lose their bad reputation in the community. The falsification of models might be the only path to scientific progress.

References

Agudelo-Toro A, Neef A. Computationally efficient simulation of electrical activity at cell membranes interacting with self-generated and externally imposed electric fields. Journal of Neural Engineering. 2013; 10(2):026019. [PubMed: 23503026]

Al-Mutawaly N, de Bruin H. Designing and constructing a magnetic stimulator: theoretical and practical considerations. Proc IEEE Eng Biol Med Eng EMBC. 2001; 23:881–884.

Al-Mutawaly N, Findlay RD. A novel coil design for magnetic nerve stimulation. Proc IEEE Can Conf Elec Comp Eng. 1998; 2:669–672.

Alavi SMM, Goetz SM, Peterchev AV. Fast curve fitting using optimal sampling. 2016 under review.

Aleman A. Use of Repetitive Transcranial Magnetic Stimulation for Treatment in Psychiatry. Clin Psychopharmacol Neurosci. 2013; 11(2):53–59. [PubMed: 24023548]

Antal A, Kincses TZ, Nitsche MA, Bartfai O, Demmer I, Sommer M, et al. Pulse configuration-dependent effects of repetitive transcranial magnetic stimulation on visual perception. NeuroReport. 2002; 13(17):2229–2223. [PubMed: 12488802]

Arai N, Okabe S, Furubayashi T, Mochizuki H, Iwata NK, Hanajima R, et al. Differences in after-effect between monophasic and biphasic high-frequency rTMS of the human motor cortex. Clinical Neurophysiology. 2007; 118(10):2227–2233. [PubMed: 17765606]

Arai N, Okabe S, Furubayashi T, Terao Y, Yuasa K, Ugawa Y. Comparison between short train, monophasic and biphasic repetitive transcranial magnetic stimulation (rTMS) of the human motor cortex. Clinical Neurophysiology. 2005; 116(3):605–613. [PubMed: 15721074]

Babyak MA. What You See May Not Be What You Get: A Brief, Nontechnical Introduction to Overfitting in Regression-Type Models. Psychosomatic Medicine. 2004; 66(3):411–421. [PubMed: 15184705]

Badcock RA, Long NJ, Mulholland M, Hellmann S, Wright A, Hamilton KA. Progress in the Manufacture of Long Length YBCO Roebel Cables. IEEE Transactions on Applied Superconductivity. 2009; 19(3):3244–3247.

Baker M, Bostock H, Grafe P, Martius P. Function and distribution of three types of rectifying channel in rat spinal root myelinated axons. The Journal of Physiology. 1987; 383:45–67. [PubMed: 2443652]

Balslev D, Braet W, McAllister C, Miall RC. Inter-individual variability in optimal current direction for transcranial magnetic stimulation of the motor cortex. Journal of Neuroscience Methods. 2007; 162(1–2):309–313. [PubMed: 17353054]

Barker AT. An Introduction to the Basic Principles of Magnetic Nerve Stimulation. Journal of Clinical Neurophysiology. 1991; 8(1):26–37. [PubMed: 2019648]

Barker, AT. The Magstim Company Ltd. Stimulators and stimulating coils for magnetically stimulating neuro-muscular tissue. US. 6,663,556. 2001.

Barker AT, Jalinous R, Freeston IL. Non-invasive magnetic stimulation of human motor cortex. The Lancet. 1985; 325(8437):1106–1107.

Basso V, Berlotti G, Infortuna A, Pasquale M. Preisach model study of the connection between magnetic and microstructural properties of soft magnetic materials. IEEE Transactions on Magnetics. 1995; 31(6):4000–4005.

Beaulieu C. Numerical data on neocortical neurons in adult rat, with special reference to the GABA population. Brain Research. 1993; 609(1–2):284–292. [PubMed: 8508310]

Beck R, Hiptmair R, Wohlmuth B. Hierarchical error estimator for eddy current computation. Numerical mathematics and advanced applications (Jyväskylä, 1999). 1999:110–120.

Bender KJ, Trussell LO. The Physiology of the Axon Initial Segment. Annual Review of Neuroscience. 2012; 35(1):249–265.

Bennie SD, Petrofsky JS, Nisperos J, Tsurudome M, Laymon M. Toward the optimal waveform for electrical stimulation of human muscle. European Journal of Applied Physiology. 2002; 88(1):13–19. [PubMed: 12436266]

Bertotti G. General properties of power losses in soft ferromagnetic materials. IEEE Transactions on Magnetics. 1988; 24(1):621–630.

Bertotti G. Dynamic generalization of the scalar Preisach model of hysteresis. IEEE Transactions on Magnetics. 1992; 28(5):2599–2601.

Bertotti G, Basso V, Pasquale M. Application of the Preisach model to the calculation of magnetization curves and power losses in ferromagnetic materials. IEEE Transactions on Magnetics. 1994; 30(2): 1052–1057.

Bestmann S, Baudewig J, Siebner HR, Rothwell JC, Frahm J. BOLD MRI responses to repetitive TMS over human dorsal premotor cortex. NeuroImage. 2005; 28(1):22–29. [PubMed: 16002305]

Beyzavi A, Nguyen NT. Modeling and optimization of planar microcoils. Journal of Micromechanics and Microengineering. 2008; 18(9):095018.

Bijsterbosch JD, Barker AT, Lee KH, Woodruff PWR. Where does transcranial magnetic stimulation (TMS) stimulate? Modelling of induced field maps for some common cortical and cerebellar targets. Medical & Biological Engineering & Computing. 2012; 50(7):671–681. [PubMed: 22678596]

Biro O, Preis K. Finite element analysis of 3-D eddy currents. IEEE Transactions on Magnetics. 1990; 26(2):418–423.

Biro O, Preis K, Buchgraber G, Ticar I. Voltage-driven coils in finite-element formulations using a current vector and a magnetic scalar potential. IEEE Transactions on Magnetics. 2004; 40(2): 1286–1289.

Blatter G, Feigel'man MV, Geshkenbein VB, Larkin AI, Vinokur VM. Vortices in high-temperature superconductors. Reviews of Modern Physics. 1994; 66(4):1125–1388.

Boglietti A, Cavagnino A, Lazzari M, Pastorelli M. Predicting iron losses in soft magnetic materials with arbitrary voltage supply: an engineering approach. IEEE Transactions on Magnetics. 2003; 39(2):981–989.

Bohning DE, Shastri A, McConnell KA, Nahas Z, Lorberbaum JP, Roberts DR, et al. A combined TMS/fMRI study of intensity-dependent TMS over motor cortex. Biological Psychiatry. 1999; 45(4):385–394. [PubMed: 10071706]

Boroojerdi B, Battaglia F, Muellbacher W, Cohen LG. Mechanisms influencing stimulus-response properties of the human corticospinal system. Clinical Neurophysiology. 2001; 112(5):931–937. [PubMed: 11336911]

Bossetti CA, Birdno MJ, Grill WM. Analysis of the quasi-static approximation for calculating potentials generated by neural stimulation. J Neural Eng. 2008; 5(1):44–53. [PubMed: 18310810]

Bostock H. The strength-duration relationship for excitation of myelinated nerve: computed dependence on membrane parameters. The Journal of Physiology. 1983; 341(1):59–74. [PubMed: 6312032]

Brouwer B, Qiao J. Characteristics and variability of lower limb motoneuron responses to transcranial magnetic stimulation. Electroencephalography and Clinical Neurophysiology/Electromyography and Motor Control. 1995; 97(1):49–54. [PubMed: 7533721]

Brunel N, van Rossum MCW. Lapicque's 1907 paper: from frogs to integrate-and-fire. Biological Cybernetics. 2007; 97(5):337–339. [PubMed: 17968583]

Buetikofer R, Lawrence PD. Electrocutaneous Nerve Stimulation-I: Model and Experiment. IEEE Transactions on Biomedical Engineering. 1978; 25(6):526–531. [PubMed: 744598]

Buetikofer R, Lawrence PD. Electrocutaneous Nerve Stimulation-II: Stimulus Waveform Selection. IEEE Transactions on Biomedical Engineering. 1979; 26(2):69–75. [PubMed: 761934]

Bugoslavsky Y, Cohen LF, Perkins GK, Polichetti M, Tate TJ, Gwilliam R, et al. Enhancement of the high-magnetic-field critical current density of superconducting MgB2 by proton irradiation. Nature. 2001; 411(6837):561–563. [PubMed: 11385564]

Bustamante V, López de Santamaría E, Marina N, Gorostiza A, Fernández Z, Gáldiz J. Neuromuscular magnetic stimulation of the quadriceps muscle after COPD exacerbations. European Respiratory Journal. 2013; 42(Suppl 57)

Bustamante VM, Gorostiza AM, López de Santa María Miró E, Iturri JBG. Magnetic Stimulation of the Quadriceps: Analysis of 2 Stimulators Used for Diagnostic and Therapeutic Applications. Archivos de Bronconeumología ((English Edition)). 2007; 43(7):411–417.

Cadwell J. Optimizing magnetic stimulator design. Electroencephalography and clinical neurophysiology Supplement. 1991; 43:238–248. [PubMed: 1773761]

Caramia MD, Cicinelli P, Paradiso C, Mariorenzi R, Zarola F, Bernardi G, et al. 'Excitability' changes of muscular responses to magnetic brain stimulation in patients with central motor disorders. Electroencephalography and Clinical Neurophysiology/Evoked Potentials Section. 1991; 81(4): 243–250.

Carroll TJ, Riek S, Carson RG. Reliability of the input–output properties of the cortico-spinal pathway obtained from transcranial magnetic and electrical stimulation. Journal of Neuroscience Methods. 2001; 112(2):193–202. [PubMed: 11716954]

Cerri G, De Leo R, Moglie F, Schiavoni A. An accurate 3-D model for magnetic stimulation of the brain cortex. Journal of Medical Engineering & Technology. 1995; 19(1):7–16. [PubMed: 7562982]

Chen M, Mogul DJ. A structurally detailed finite element human head model for simulation of transcranial magnetic stimulation. Journal of Neuroscience Methods. 2009; 179(1):111–120. [PubMed: 19428517]

Claus D, Murray NMF, Spitzer A, Flügel D. The influence of stimulus type on the magnetic excitation of nerve structures. Electroencephalography and Clinical Neurophysiology. 1990; 75(4):342–349. [PubMed: 1691083]

Clemens M, Wilke M, Weiland T. Advanced FI2TD algorithms for transient eddy current problems. COMPEL – The international journal for computation and mathematics in electrical and electronic engineering. 2001; 20(2):365–379.

Cohen LG, Roth BJ, Nilsson J, Dang N, Panizza M, Bandinelli S, et al. Effects of coil design on delivery of focal magnetic stimulation. Technical considerations. Electroencephalography and Clinical Neurophysiology. 1990; 75(4):350–357. [PubMed: 1691084]

Comeau, R. Neuronavigation for Transcranial Magnetic Stimulation. In: Rotenberg, A.Horvath, CJ., Pascual-Leone, A., editors. Transcranial Magnetic Stimulation. New York, NY: Springer New York; 2014. p. 31-56.

Cona F, Zavaglia M, Massimini M, Rosanova M, Ursino M. A neural mass model of interconnected regions simulates rhythm propagation observed via TMS-EEG. NeuroImage. 2011; 57(3):1045–1058. [PubMed: 21600291]

Corthout E, Barker A, Cowey A. Transcranial magnetic stimulation. Which part of the current waveform causes the stimulation? Experimental Brain Research. 2001; 141(1):128–132. [PubMed: 11685417]

Counter SA. Auditory brainstem and cortical responses following extensive transcranial magnetic stimulation. Journal of the Neurological Sciences. 1994; 124(2):163–170. [PubMed: 7964867]

Counter SA, Borg E. Analysis of the coil generated impulse noise in extracranial magnetic stimulation. Electroencephalography and Clinical Neurophysiology/Evoked Potentials Section. 1992; 85(4): 280–288.

Counter SA, Borg E, Lofqvist L. Acoustic trauma in extracranial magnetic brain stimulation. Electroencephalography and Clinical Neurophysiology. 1991; 78(3):173–184. [PubMed: 1707789]

Crowther LJ, Marketos P, Williams PI, Melikhov Y, Jiles DC, Starzewski JH. Transcranial magnetic stimulation: Improved coil design for deep brain investigation. Journal of Applied Physics. 2011; 109(7):07B314.

d'Aloja G, Lino P, Maione B, Rizzo A. Nonlinear Modeling of Brain Motor Waves via Transcranial Magnetic Stimulation. IEEE Proc Conf on Decision and Control. 2005; 44:4833–4938.

D'Ostilio K, Goetz SM, Ciocca M, Chieffo R, Chen J-CA, Peterchev AV, et al. Effect of coil orientation on strength-duration time constant with controllable pulse parameter transcranial magnetic stimulation. Clinical Neurophysiology. 2014; 125(Suppl 1):S123.

D'Ostilio K, Goetz SM, Hannah R, Ciocca M, Chieffo R, Chen JCA, et al. Effect of coil orientation on strength–duration time constant and I-wave activation with controllable pulse parameter transcranial magnetic stimulation. Clinical Neurophysiology. 2016; 127(1):675–683. [PubMed: 26077634]

d'Aloja, G., Lino, P., Maione, B., Rizzo, A. Modeling of Motor Neuronal Structures Via Transcranial Magnetic Stimulation. In: Filipe, J.Ferrier, J-L.Cetto, JA., Carvalho, M., editors. Informatics in Control, Automation and Robotics II. Dordrecht: Springer Netherlands; 2007. p. 191-197.

Darling WG, Wolf SL, Butler AJ. Variability of motor potentials evoked by transcranial magnetic stimulation depends on muscle activation. Experimental Brain Research. 2006; 174(2):376–385. [PubMed: 16636787]

Davey K, Epstein CM. Magnetic stimulation coil and circuit design. IEEE Transactions on Biomedical Engineering. 2000; 47(11):1493–1499. [PubMed: 11077743]

Davey K, Epstein CM, George MS, Bohning DE. Modeling the effects of electrical conductivity of the head on the induced electric field in the brain during magnetic stimulation. Clinical Neurophysiology. 2003; 114(11):2204–2209. [PubMed: 14580620]

Davey K, Riehl M. Designing transcranial magnetic stimulation systems. IEEE Transactions on Magnetics. 2005; 41(3):1142–1148.

Davey KR, Riehl ME. Suppressing the surface field during transcranial magnetic stimulation. IEEE Trans Biomed Eng. 2006; 53(2):190–194. [PubMed: 16485747]

de Boer R, Vrooman HA, Ikram MA, Vernooij MW, Breteler MMB, van der Lugt A, et al. Accuracy and reproducibility study of automatic MRI brain tissue segmentation methods. NeuroImage. 2010; 51(3):1047–1056. [PubMed: 20226258]

De Geeter N, Crevecoeur G, Dupre L. An Efficient 3-D Eddy-Current Solver Using an Independent Impedance Method for Transcranial Magnetic Stimulation. IEEE Transactions on Biomedical Engineering. 2011; 58(2):310–320. [PubMed: 20959261]

De Geeter N, Crevecoeur G, Dupré L, Van Hecke W, Leemans A. A DTI-based model for TMS using the independent impedance method with frequency-dependent tissue parameters. Physics in Medicine and Biology. 2012; 57(8):2169. [PubMed: 22452983]

De Geeter N, Crevecoeur G, Leemans A, Dupré L. Effective electric fields along realistic DTI-based neural trajectories for modelling the stimulation mechanisms of TMS. Physics in Medicine and Biology. 2015; 60(2):453. [PubMed: 25549237]

De Lucia M, Parker GJM, Embleton K, Newton JM, Walsh V. Diffusion tensor MRI-based estimation of the influence of brain tissue anisotropy on the effects of transcranial magnetic stimulation. NeuroImage. 2007; 36(4):1159–1170. [PubMed: 17524673]

Dean D, Lawrence PD. Optimization of Neural Stimuli Based Upon a Variable Threshold Potential. IEEE Transactions on Biomedical Engineering. 1985; BME-32(1):8–14.

Deng ZD, Lisanby SH, Peterchev AV. Electric field strength and focality in electroconvulsive therapy and magnetic seizure therapy: a finite element simulation study. J Neural Eng. 2011; 8(1):016007. [PubMed: 21248385]

Deng ZD, Lisanby SH, Peterchev AV. Electric field depth–focality tradeoff in transcranial magnetic stimulation: Simulation comparison of 50 coil designs. Brain Stimulation. 2013; 6(1):1–13. [PubMed: 22483681]

Deng ZD, Lisanby SH, Peterchev AV. Coil design considerations for deep transcranial magnetic stimulation. Clin Neurophysiol. 2014; 125(6):1202–1212. [PubMed: 24411523]

Deng ZD, Lisanby SH, Peterchev AV. Effect of Anatomical Variability on Electric Field Characteristics of Electroconvulsive Therapy and Magnetic Seizure Therapy: A Parametric Modeling Study. IEEE Transactions on Neural Systems and Rehabilitation Engineering. 2015; 23(1):22–31. [PubMed: 25055384]

Deng ZD, Peterchev AV, Lisanby SH. Coil design considerations for deep-brain transcranial magnetic stimulation (dTMS). Proc IEEE Eng Biol Med Conf EMBC. 2008; 30:5675–5679.

Devanne H, Lavoie AB, Capaday C. Input-output properties and gain changes in the human corticospinal pathway. Experimental Brain Research. 1997; 114(2):329–338. [PubMed: 9166922]

Di Lazzaro V, Oliviero A, Pilato F, Saturno E, Dileone M, Mazzone P, et al. The physiological basis of transcranial motor cortex stimulation in conscious humans. Clinical Neurophysiology. 2004; 115(2):255–266. [PubMed: 14744565]

Di Lazzaro V, Profice P, Ranieri F, Capone F, Dileone M, Oliviero A, et al. I-wave origin and modulation. Brain Stimulation. 2012; 5(4):512–525. [PubMed: 21962980]

Di Lazzaro V, Ziemann U, Lemon RN. State of the art: Physiology of transcranial motor cortex stimulation. Brain Stimulation. 2008; 1(4):345–362. [PubMed: 20633393]

Drummond C, Japkowicz N. Warning: statistical benchmarking is addictive. Kicking the habit in machine learning. Journal of Experimental & Theoretical Artificial Intelligence. 2010; 22(1):67–80.

Durand D, Ferguson AS, Dalbasti T. Induced electric fields by magnetic stimulation in non-homogeneous conducting media. Proc IEEE Eng Biol Med Conf EMBC. 1989; 11:1252–1253.

Eggert LD, Sommer J, Jansen A, Kircher T, Konrad C. Accuracy and Reliability of Automated Gray Matter Segmentation Pathways on Real and Simulated Structural Magnetic Resonance Images of the Human Brain. PLoS ONE. 2012; 7(9):e45081. [PubMed: 23028771]

Eldaief MC, Press DZ, Pascual-Leone A. Transcranial magnetic stimulation in neurology: A review of established and prospective applications. Neurology Clinical Practice. 2013; 3(6):519–526. [PubMed: 24353923]

Ellaway PH, Davey NJ, Maskill DW, Rawlinson SR, Lewis HS, Anissimova NP. Variability in the amplitude of skeletal muscle responses to magnetic stimulation of the motor cortex in man. Electroencephalography and Clinical Neurophysiology/Electromyography and Motor Control. 1998; 109(2):104–113. [PubMed: 9741800]

Emrich D, Fischer A, Altenhöfer C, Weyh T, Helling F, Goetz S, et al. Muscle force development after low-frequency magnetic burst stimulation in dogs. Muscle & Nerve. 2012; 46(6):951–953. [PubMed: 23225386]

Epstein, CM., Davey, KR. Emory University. Apparatus and method for transcranial magnetic brain stimulation, including the treatment of depression and the localization and characterization of speech arrest. US. 6,425,852. 1994.

Epstein CM, Davey KR. Iron-Core Coils for Transcranial Magnetic Stimulation. Journal of Clinical Neurophysiology. 2002; 19(4):376–381. [PubMed: 12436092]

Esselle KP, Stuchly MA. Neural stimulation with magnetic fields: analysis of induced electric fields. IEEE Transactions on Biomedical Engineering. 1992; 39(7):693–700. [PubMed: 1516936]

Esser SK, Hill SL, Tononi G. Modeling the Effects of Transcranial Magnetic Stimulation on Cortical Circuits. Journal of Neurophysiology. 2005; 94(1):622–639. [PubMed: 15788519]

Fang ZP, Mortimer JT. Selective activation of small motor axons by quasitrapezoidal current pulses. Biomedical Engineering, IEEE Transactions on. 1991; 38(2):168–174.

Fanjul-Vélez F, Salas-García I, Ortega-Quijano N, Arce-Diego JL. FDTD-based Transcranial Magnetic Stimulation model applied to specific neurodegenerative disorders. Computer Methods and Programs in Biomedicine. 2015; 118(1):34–43. [PubMed: 25453382]

FitzHugh R. Impulses and Physiological States in Theoretical Models of Nerve Membrane. Biophysical Journal. 1961; 1(6):445–466. [PubMed: 19431309]

Freeman SA, Desmazières A, Fricker D, Lubetzki C, Sol-Foulon N. Mechanisms of sodium channel clustering and its influence on axonal impulse conduction. Cellular and Molecular Life Sciences. 2016; 73(4):723–735. [PubMed: 26514731]

Friedman, A., Wolfus, S., Yeshurun, Y., Bar-Haim, Z. Bar Ilan University, Ricor Cryogenic & Vacuum Systems. Method for manufacturing superconducting coils. US. 11/239,380. 2004.

Fung PK, Haber AL, Robinson PA. Neural field theory of plasticity in the cerebral cortex. Journal of Theoretical Biology. 2013; 318:44–57. [PubMed: 23036915]

Gabriel C, Peyman A, Grant EH. Electrical conductivity of tissue at frequencies below 1 MHz. Physics in Medicine and Biology. 2009; 54(16):4863. [PubMed: 19636081]

Gabriel S, Lau RW, Gabriel C. The dielectric properties of biological tissues: II. Measurements in the frequency range 10 Hz to 20 GHz. Physics in Medicine and Biology. 1996; 41(11):2251. [PubMed: 8938025]

Ge S, Wang JP, Tang HY, Xiao X, Wu W. A Design of Array Transcranial Magnetic Stimulation Coil System. International Journal of Medical, Health, Biomedical, Bioengineering and Pharmaceutical Engineering. 2012; 6(5):160–163.

Gentet LJ, Stuart GJ, Clements JD. Direct Measurement of Specific Membrane Capacitance in Neurons. Biophysical Journal. 2000; 79(1):314–320. [PubMed: 10866957]

Ghiron, KM., Riehl, ME. Neuronetics, Inc. Ferrofluidic cooling and acoustical noise reduction in magnetic stimulators. US. 7,396,326. 2005.

Ghiron, KM., Riehl, ME., Shipway, IM. Neuronetics, Inc. Magnetic stimulation coils and ferromagnetic components for reduced surface stimulation and improved treatment depth. US. 2015/0196772. 2014.

Gilbert TL. A phenomenological theory of damping in ferromagnetic materials. IEEE Transactions on Magnetics. 2004; 40(6):3443–3449.

Goetz SM, Afinowi IA, Herzog HG, Weyh T. Coil Design for Neuromuscular Magnetic Stimulation Based on a Detailed 3D Thigh Model. IEEE Transaction on Magnetics. 2013; 50(6):1–10.

Goetz SM, Herzog HG, Gattinger N, Gleich B. Comparison of coil designs for peripheral magnetic muscle stimulation. Journal of Neural Engineering. 2011; 8(5):056007. [PubMed: 21832812]

Goetz, SM., Li, Z., Liang, X., Zhang, C., Lukic, S., Peterchev, AV. Sensorless scheduling of the modular multilevel series-parallel converter: enabling a flexible, efficient, modular battery. IEEE Applied Power Electronics Conference APEC; 2016. p. 2349-2354.

Goetz SM, Lisanby SH, Murphy DLK, Price RJ, O'Grady G, Peterchev AV. Impulse Noise of Transcranial Magnetic Stimulation: Measurement, Safety, and Auditory Neuromodulation. Brain Stimulation: Basic, Translational, and Clinical Research in Neuromodulation. 2015; 8(1):161–163.

Goetz SM, Luber B, Lisanby SH, Murphy DL, Kozyrkov CI, Grill WM, et al. Enhancement of neuromodulation with novel pulse shapes generated by controllable pulse parameter transcranial magnetic stimulation. Brain Stimulation. 2016; 9(1):39–47. [PubMed: 26460199]

Goetz SM, Luber B, Lisanby SH, Peterchev AV. Dual-source variability model for estimating and predicting brain-stimulation-evoked responses. Brain Stimulation. 2014; 7(4):541–552. [PubMed: 24794287]

Goetz SM, Murphy DLK, Peterchev AV. Transcranial Magnetic Stimulation Device With Reduced Acoustic Noise. IEEE Magnetics Letters. 2014; 5:1–4.

Goetz SM, Peterchev AV. A model of variability in brain stimulation evoked responses. Proc IEEE Eng Biol Med Conf EMBC. 2012; 34:6434–6437.

Goetz SM, Peterchev AV, Weyh T. Modular Multilevel Converter With Series and Parallel Module Connectivity: Topology and Control. Power Electronics, IEEE Transactions on. 2015; 30(1):203–215.

Goetz SM, Pfaeffl M, Huber J, Singer M, Marquardt R, Weyh T. Circuit topology and control principle for a first magnetic stimulator with fully controllable waveform. Proc IEEE Eng Biol Med Conf EMBC. 2012; 34:4700–4703.

Goetz SM, Truong CN, Gerhofer MG, Peterchev AV, Herzog HG, Weyh T. Analysis and Optimization of Pulse Dynamics for Magnetic Stimulation. PLoS ONE. 2013; 8(3):e55771. [PubMed: 23469168]

Goetz SM, Truong NC, Gerhofer MG, Peterchev AV, Herzog H, Weyh T. Optimization of magnetic neurostimulation waveforms for minimum power loss. IEEE EMBC. 2012; 34:4652–4655.

Goetz SM, Weyh T, Herzog HG. Analysis of a novel magnetic stimulation system: Magnetic harmonic multi-cycle stimulation (MHMS). Proc IEEE Conf Biomed Pharm Eng. 2009:1–6.

Goetz SM, Whiting P, Peterchev AV. Threshold estimation with transcranial magnetic stimulation: algorithm comparison. Clinical Neurophysiology. 2011; 122(S1):197.

Golestanirad L, Mattes M, Mosig JR, Pollo C. Effect of Model Accuracy on the Result of Computed Current Densities in the Simulation of Transcranial Magnetic Stimulation. IEEE Transactions on Magnetics. 2010; 46(12):4046–4051.

Gomez L, Cajko F, Hernandez-Garcia L, Grbic A, Michielssen E. Numerical Analysis and Design of Single-Source Multicoil TMS for Deep and Focused Brain Stimulation. IEEE Transactions on Biomedical Engineering. 2013; 60(10):2771–2782. [PubMed: 23708768]

Gomez LJ, Yücel AC, Hernandez-Garcia L, Taylor SF, Michielssen E. Uncertainty Quantification in Transcranial Magnetic Stimulation via High-Dimensional Model Representation. IEEE Transactions on Biomedical Engineering. 2015; 62(1):361–372. [PubMed: 25203980]

Goodwin BD, Butson CR. Subject-Specific Multiscale Modeling to Investigate Effects of Transcranial Magnetic Stimulation. Neuromodulation: Technology at the Neural Interface. 2015; 18(8):694–704.

Gorman PH, Mortimer JT. The Effect of Stimulus Parameters on the Recruitment Characteristics of Direct Nerve Stimulation. Biomedical Engineering, IEEE Transactions on. 1983; BME-30(7): 407–414.

Grill WM, Mortimer JT. Stimulus waveforms for selective neural stimulation. Engineering in Medicine and Biology Magazine, IEEE. 1995; 14(4):375–385.

Gugino LD, Rafael Romero J, Aglio L, Titone D, Ramirez M, Pascual-Leone A, et al. Transcranial magnetic stimulation coregistered with MRI: a comparison of a guided versus blind stimulation technique and its effect on evoked compound muscle action potentials. Clinical Neurophysiology. 2001; 112(10):1781–1792. [PubMed: 11595135]

Guidi M, Scarpino O, Angeleri F, Antili R, Leo Rd. Brain cortex stimulation by using magnetic pulses: analysis of the induced current distribution by means of a computer simulated model. Proc IEEE Eng Biol Med Conf (EMBC). 1989; 11:1169–1171.

Gutfleisch O, Willard MA, Brück E, Chen CH, Sankar SG, Liu JP. Magnetic Materials and Devices for the 21st Century: Stronger, Lighter, and More Energy Efficient. Advanced Materials. 2011; 23(7):821–842. [PubMed: 21294168]

Haiji H, Okada K, Hiratani T, Abe M, Ninomiya M. Magnetic properties and workability of 6.5% Si steel sheet. Journal of Magnetism and Magnetic Materials. 1996; 160:109–114.

Han BH, Chun IK, Lee SC, Lee SY. Multichannel magnetic stimulation system design considering mutual couplings among the stimulation coils. IEEE Transactions on Biomedical Engineering. 2004; 51(5):812–817. [PubMed: 15132507]

Hannah R, Ciocca M, Sommer M, Hammond P, Rothwell JC. Continuous theta burst stimulation with monophasic pulses: effect of current direction. Clinical Neurophysiology. 2014; 125(1):S332–S333.

Havel WJ, Nyenhuis JA, Bourland JD, Foster KS, Geddes LA, Graber GP, et al. Comparison of rectangular and damped sinusoidal dB/dt waveforms in magnetic stimulation. IEEE Transactions on Magnetics. 1997; 33(5):4269–4271.

Hawkins DM, Kraker J. Deterministic fallacies and model validation. Journal of Chemometrics. 2010; 24(3–4):188–193.

He ZZ, Liu J. Anisotropic subvoxel-smooth conduction model for bioelectromagnetism analysis. Journal of Applied Physics. 2016; 119(2):024701.

Heller L, van Hulsteyn DB. Brain stimulation using electromagnetic sources: theoretical aspects. Biophys J. 1992; 63(1):129–138. [PubMed: 1420862]

Hindmarsh JL, Rose RM. A Model of Neuronal Bursting Using Three Coupled First Order Differential Equations. Proceedings of the Royal Society of London B: Biological Sciences. 1984; 221(1222): 87–102. [PubMed: 6144106]

Ho SL, Xu G, Fu WN, Yang Q, Hou H, Yan W. Optimization of Array Magnetic Coil Design for Functional Magnetic Stimulation Based on Improved Genetic Algorithm. IEEE Transactions on Magnetics. 2009; 45(10):4849–4852.

Hodgkin AL, Huxley AF. A quantitative description of membrane current and its application to conduction and excitation in nerve. The Journal of Physiology. 1952; 117(4):500–544. [PubMed: 12991237]

Hollaus K, Biro O. A FEM formulation to treat 3D eddy currents in laminations. IEEE Transactions on Magnetics. 2000; 36(4):1289–1292.

Howard CQ, Hansen CH, Zander AC. A review of current ultrasound exposure limits. J Occup Health Safety. 2005; 1:253–257.

Howell B, Medina LE, Grill WM. Effects of frequency-dependent membrane capacitance on neural excitability. Journal of Neural Engineering. 2015; 12(5):056015. [PubMed: 26348707]

Huang YZ, Rothwell JC, Chen RS, Lu CS, Chuang WL. The theoretical model of theta burst form of repetitive transcranial magnetic stimulation. Clinical Neurophysiology. 2011; 122(5):1011–1018. [PubMed: 20869307]

Hussennether V, Oomen M, Leghissa M, Neumüller HW. DC and AC properties of Bi-2223 cabled conductors designed for high-current applications. Physica C: Superconductivity. 2004; 401(1–4):135–139.

Ilmoniemi, R., Koponen, L., Nieminen, J., Järneflt, G. Nexstim Oy. MTMS coil device with overlapping coil windings. US. 2014/0357935. 2014.

Ilmoniemi, R., Ruohonen, J., Kamppuri, J., Virtanen, J. Nexstim. Stimulator head and method for attenuating the sound emitted by a stimulator coil. US. 6,503,187. 1997.

Ilmoniemi, RJ., Koponen, LM., Nieminen, JO., Järnefelt, G. Nexstim Oy. mTMS coil device with overlapping coil windings. US. 14/294,573. 2013.

Im CH, Lee C. Computer-Aided Performance Evaluation of a Multichannel Transcranial Magnetic Stimulation System. IEEE Transactions on Magnetics. 2006; 42(12):3803–3808.

Izhikevich EM. Simple model of spiking neurons. IEEE Transactions on Neural Networks. 2003; 14(6):1569–1572. [PubMed: 18244602]

Izhikevich EM. Which model to use for cortical spiking neurons? IEEE Transactions on Neural Networks. 2004; 15(5):1063–1070. [PubMed: 15484883]

Jackson, JD. Classical Electrodynamics. 3. New York: John Wiley & Sons, Inc; 1999.

Jalinous R. Technical and Practical Aspects of Magnetic Nerve Stimulation. Journal of Clinical Neurophysiology. 1991; 8(1):10–25. [PubMed: 2019644]

Janssen AM, Oostendorp TF, Stegeman DF. The coil orientation dependency of the electric field induced by TMS for M1 and other brain areas. J Neuroeng Rehabil. 2015; 12(47)

Janssen AM, Rampersad SM, Lucka F, Lanfer B, Lew S, ÜA, et al. The influence of sulcus width on simulated electric fields induced by transcranial magnetic stimulation. Physics in Medicine and Biology. 2013; 58(14):4881. [PubMed: 23787706]

Jezernik S, Sinkjaer T, Morari M. Charge and energy minimization in electrical/magnetic stimulation of nervous tissue. Journal of Neural Engineering. 2010; 7(4):046004. [PubMed: 20551509]

Jiles, D. Introduction to magnetism and magnetic materials. 3. Boca Raton (FL): CRC Press; 2016.

Jiles DC, Atherton DL. Theory of ferromagnetic hysteresis. Journal of Magnetism and Magnetic Materials. 1986; 61(1):48–60.

Julkunen P, Ruohonen J, Sääskilahti S, Säisänen L, Karhu J. Threshold curves for transcranial magnetic stimulation to improve reliability of motor pathway status assessment. Clinical Neurophysiology. 2011; 122(5):975–983. [PubMed: 20888291]

Kaelin-Lang A, Cohen LG. Enhancing the quality of studies using transcranial magnetic and electrical stimulation with a new computer-controlled system. Journal of Neuroscience Methods. 2000; 102(1):81–89. [PubMed: 11000414]

Kaelin-Lang A, Luft AR, Sawaki L, Burstein AH, Sohn YH, Cohen LG. Modulation of human corticomotor excitability by somatosensory input. The Journal of Physiology. 2002; 540(2):623–633. [PubMed: 11956348]

Kamitani Y, Bhalodia VM, Kubota Y, Shimojo S. A model of magnetic stimulation of neocortical neurons. Neurocomputing. 2001; 38–40:697–703.

Kammer T, Beck S, Thielscher A, Laubis-Herrmann U, Topka H. Motor thresholds in humans: a transcranial magnetic stimulation study comparing different pulse waveforms, current directions and stimulator types. Clinical Neurophysiology. 2001; 112(2):250–258. [PubMed: 11165526]

Kammer T, Vorwerg M, Herrnberger B. Anisotropy in the visual cortex investigated by neuronavigated transcranial magnetic stimulation. NeuroImage. 2007; 36(2):313–321. [PubMed: 17442592]

Kim DH, Loukaides N, Sykulski JK, Georghious GE. Numerical investigation of the electric field distribution induced in the brain by transcranial magnetic stimulation. IEE Proc Sci Meas Tech. 2004; 151(6):479–483.

Klauschen F, Goldman A, Barra V, Meyer-Lindenberg A, Lundervold A. Evaluation of automated brain MR image segmentation and volumetry methods. Human Brain Mapping. 2009; 30(4): 1310–1327. [PubMed: 18537111]

Knäulein R, Weyh T. Minimization of energy stored in the magnetic field of air coils for medical application. Int Workshop on electric and magnetic fields Liege. 1996; 3:477–482.

Kole MHP, Ilschner SU, Kampa BM, Williams SR, Ruben PC, Stuart GJ. Action potential generation requires a high sodium channel density in the axon initial segment. Nat Neurosci. 2008; 11(2): 178–186. [PubMed: 18204443]

Kole, Maarten HP., Stuart, Greg J. Signal Processing in the Axon Initial Segment. Neuron. 2012; 73(2):235–247. [PubMed: 22284179]

Koponen LM, Nieminen JO, Ilmoniemi RJ. Minimum-energy Coils for Transcranial Magnetic Stimulation: Application to Focal Stimulation. Brain Stimulation. 2015; 8(1):124–134. [PubMed: 25458713]

Krings A, Soulard J. Overview and Comparison of Iron Loss Models for Electrical Machines. Proc Int Conf Exhib on Ecol Vehicles and Renewable Energies (EVER 10). 2010:5.

Krings T, Buchbinder BR, Butler WE, Chiappa KH, Jiang HJ, Rosen BR, et al. Stereotactic Transcranial Magnetic Stimulation: Correlation with Direct Electrical Cortical Stimulation. Neurosurgery. 1997; 41(6):1319–1326. [PubMed: 9402583]

Krishnan AV, Lin CSY, Park SB, Kiernan MC. Axonal ion channels from bench to bedside: A translational neuroscience perspective. Progress in Neurobiology. 2009; 89(3):288–313. [PubMed: 19699774]

Laakso I, Hirata A. Fast multigrid-based computation of the induced electric field for transcranial magnetic stimulation. Physics in Medicine and Biology. 2012; 57(23):7753. [PubMed: 23128377]

Laakso I, Hirata A, Ugawa Y. Effects of coil orientation on the electric field induced by TMS over the hand motor area. Physics in Medicine and Biology. 2014; 59(1):203. [PubMed: 24334481]

Lai HC, Jan LY. The distribution and targeting of neuronal voltage-gated ion channels. Nat Rev Neurosci. 2006; 7(7):548–562.doi: 10.1038/nrn1938 [PubMed: 16791144]

Landau LD, Lifshitz E. On the theory of the dispersion of magnetic permeability in ferromagnetic bodies. Phys Z Sowjetunion. 1935; 8(153):101–114.

Langley P. Machine Learning as an Experimental Science. Machine Learning. 1988; 3(1):5–8.

Lapicque L. Recherches quantatives sur l'excitation électrique des nerfs traitée comme une polarisation. Journal de Physiologie et de Pathologie Générale. 1907; 9:620–635.

Larbalestier D, Gurevich A, Feldmann DM, Polyanskii A. High-Tc superconducting materials for electric power applications. Nature. 2001; 414(6861):368–377. [PubMed: 11713544]

Laudani A, Fulginei FR, Salvini A. TMS Array Coils Optimization by Means of CFSO. IEEE Transactions on Magnetics. 2015; 51(3):1–4. [PubMed: 26203196]

Lee WH, Deng ZD, Kim TS, Laine AF, Lisanby SH, Peterchev AV. Regional electric field induced by electroconvulsive therapy in a realistic finite element head model: Influence of white matter anisotropic conductivity. NeuroImage. 2012; 59(3):2110–2123. [PubMed: 22032945]

Lee WH, Lisanby SH, Laine AF, Peterchev AV. Stimulation strength and focality of electroconvulsive therapy and magnetic seizure therapy in a realistic head model. Proc IEEE Eng Biol Med Conf (EMBC). 2014; 36:410–413.

Lee WH, Lisanby SH, Laine AF, Peterchev AV. Comparison of electric field strength and spatial distribution of electroconvulsive therapy and magnetic seizure therapy in a realistic human head model. European Psychiatry. 2016; 36:55–64. [PubMed: 27318858]

Leterrier C, Brachet A, Dargent B, Vacher H. Determinants of voltage-gated sodium channel clustering in neurons. Seminars in Cell & Developmental Biology. 2011; 22(2):171–177. [PubMed: 20934527]

Leterrier C, Brachet A, Fache MP, Dargent B. Voltage-gated sodium channel organization in neurons: Protein interactions and trafficking pathways. Neuroscience Letters. 2010; 486(2):92–100. [PubMed: 20817077]

Littmann MF. Structures and Magnetic Properties of Grain-Oriented 3.2% Silicon—Iron. Journal of Applied Physics. 1967; 38(3):1104–1108.

Lloberas J, Sumper A, Sanmarti M, Granados X. A review of high temperature superconductors for offshore wind power synchronous generators. Renewable and Sustainable Energy Reviews. 2014; 38:404–414.

Long NJ, Badcock R, Beck P, Mulholl M, Ross N, Staines M, et al. Narrow strand YBCO Roebel cable for lowered AC loss. Journal of Physics: Conference Series. 2008; 97(1):012280.

Loo C, Sachdev P, Elsayed H, McDarmont B, Mitchell P, Wilkinson M, et al. Effects of a 2- to 4-week course of repetitive transcranial magnetic stimulation (rTMS) on neuropsychologic functioning,

electroencephalogram, and auditory threshold in depressed patients. Biological Psychiatry. 2001; 49(7):615–623. [PubMed: 11297719]

Lorenzen HW, Weyh T. Practical application of the summation method for 3-D static magnetic field calculation of a setup of conductive and ferromagnetic material. IEEE Transactions on Magnetics. 1992; 28(2):1481–1484.

Maccabee PJ, Amassian VE, Cracco RQ, Cadwell JA. An analysis of peripheral motor nerve stimulation in humans using the magnetic coil. Electroencephalography and Clinical Neurophysiology. 1988; 70(6):524–533. [PubMed: 2461286]

Maccabee PJ, Nagarajan SS, Amassian VE, Durand DM, Szabo AZ, Ahad AB, et al. Influence of pulse sequence, polarity and amplitude on magnetic stimulation of human and porcine peripheral nerve. The Journal of Physiology. 1998; 513(2):571–585. [PubMed: 9807005]

Maeda H, Yanagisawa Y. Recent Developments in High-Temperature Superconducting Magnet Technology (Review). IEEE Transactions on Applied Superconductivity. 2014; 24(3):1–12.

Magistris MR, Rösler KM, Truffert A, Landis T, Hess CW. A clinical study of motor evoked potentials using a triple stimulation technique. Brain. 1999; 122(2):265–279. [PubMed: 10071055]

Magistris MR, Rösler KM, Truffert A, Myers JP. Transcranial stimulation excites virtually all motor neurons supplying the target muscle. A demonstration and a method improving the study of motor evoked potentials. Brain. 1998; 121(3):437–450. [PubMed: 9549520]

Malcolm MP, Triggs WJ, Light KE, Shechtman O, Khandekar G, Gonzalez Rothi LJ. Reliability of motor cortex transcranial magnetic stimulation in four muscle representations. Clinical Neurophysiology. 2006; 117(5):1037–1046. [PubMed: 16564206]

Maxwell, JC. A Treatise on Electricity and Magnetism. 3. Oxford: Clarendon Press; 1891.

McIntyre CC, Richardson AG, Grill WM. Modeling the Excitability of Mammalian Nerve Fibers: Influence of Afterpotentials on the Recovery Cycle. Journal of Neurophysiology. 2002; 87(2): 995–1006. [PubMed: 11826063]

McNeal DR. Analysis of a Model for Excitation of Myelinated Nerve. IEEE Transactions on Biomedical Engineering. 1976; BME-23(4):329–337.

McRobbie D. Design and instrumentation of a magnetic nerve stimulator. Journal of Physics E: Scientific Instruments. 1985; 18(1):74.

Mills KR, Boniface SJ, Schubert M. Magnetic brain stimulation with a double coil: the importance of coil orientation. Electroencephalography and Clinical Neurophysiology/Evoked Potentials Section. 1992; 85(1):17–21.

Miranda PC, Hallett M, Basser PJ. The electric field induced in the brain by magnetic stimulation: a 3-D finite-element analysis of the effect of tissue heterogeneity and anisotropy. IEEE Transactions on Biomedical Engineering. 2003; 50(9):1074–1085. [PubMed: 12943275]

Miranda PC, Lomarev M, Hallett M. Modeling the current distribution during transcranial direct current stimulation. Clinical Neurophysiology. 2006; 117(7):1623–1629. [PubMed: 16762592]

Mitchell WK, Baker MR, Baker SN. Muscle responses to transcranial stimulation in man depend on background oscillatory activity. The Journal of Physiology. 2007; 583(2):567–579. [PubMed: 17627997]

Moffitt MA, McIntyre CC, Grill WM. Prediction of myelinated nerve fiber stimulation thresholds: limitations of linear models. Biomedical Engineering, IEEE Transactions on. 2004; 51(2):229–236.

Moisa M, Pohmann R, Ewald L, Thielscher A. New coil positioning method for interleaved transcranial magnetic stimulation (TMS)/functional MRI (fMRI) and its validation in a motor cortex study. Journal of Magnetic Resonance Imaging. 2009; 29(1):189–197. [PubMed: 19097080]

Moosavi SH, Ellaway PH, Catley M, Stokes MJ, Haque N. Corticospinal function in severe brain injury assessed using magnetic stimulation of the motor cortex in man. Journal of the Neurological Sciences. 1999; 164(2):179–186. [PubMed: 10402031]

Möser, M., Kropp, W. Körperschall [Structure-Borne Sound]. Berlin/New York: Springer; 2010.

Mould, S. Magstim Company Limited. Coil assemblies for magnetic stimulators. US. 6,179,770. 1998.

Mueller JK, Grigsby EM, Prevosto V, Petraglia FW Iii, Rao H, Deng ZD, et al. Simultaneous transcranial magnetic stimulation and single-neuron recording in alert non-human primates. Nat Neurosci. 2014; 17(8):1130–1136. [PubMed: 24974797]

Nadeem M, Thorlin T, Gandhi OP, Persson M. Computation of electric and magnetic stimulation in human head using the 3-D impedance method. IEEE Transactions on Biomedical Engineering. 2003; 50(7):900–907. [PubMed: 12848358]

Nagumo J, Arimoto S, Yoshizawa S. An Active Pulse Transmission Line Simulating Nerve Axon. Proceedings of the IRE. 1962; 50(10):2061–2070.

Navarro de Lara LI, Windischberger C, Kuehne A, Woletz M, Sieg J, Bestmann S, et al. A novel coil array for combined TMS/fMRI experiments at 3 T. Magnetic Resonance in Medicine. 2015; 74(5):1492–1501. [PubMed: 25421603]

Navarro de Lara, LI., Windischberger, C., Laistler, E., Sieg, J., Moser, E., Kühne, A. Medical University of Vienna. Method and system for combined transcranial magnetic stimulation (TMS) and functional magnetic resonance imaging (fMRI) studies. US. 2015/0099963. 2013.

Ni Z, Charab S, Gunraj C, Nelson AJ, Udupa K, Yeh IJ, et al. Transcranial Magnetic Stimulation in Different Current Directions Activates Separate Cortical Circuits. Journal of Neurophysiology. 2011; 105(2):749–756. [PubMed: 21148098]

Niehaus L, Meyer BU, Weyh T. Influence of pulse configuration and direction of coil current on excitatory effects of magnetic motor cortex and nerve stimulation. Clinical Neurophysiology. 2000; 111(1):75–80. [PubMed: 10656513]

Nielsen JF. Logarithmic Distribution of Amplitudes of Compound Muscle Action Potentials Evoked by Transcranial Magnetic Stimulation. Journal of Clinical Neurophysiology. 1996; 13(5):423–434. [PubMed: 8897207]

Nielsen JF, Klemar B, Kiilerich H. A New High-Frequency Magnetic Stimulator with an Oil-Cooled Coil. Journal of Clinical Neurophysiology. 1995; 12(5):460–467. [PubMed: 8576391]

Nikouline V, Ruohonen J, Ilmoniemi RJ. The role of the coil click in TMS assessed with simultaneous EEG. Clinical Neurophysiology. 1999; 110(8):1325–1328. [PubMed: 10454266]

Nowak GL, Bullier J. Axons, but not cell bodies, are activated by electrical stimulation in cortical gray matter I. Evidence from chronaxie measurements. Experimental Brain Research. 1998a; 118(4): 477–488. [PubMed: 9504843]

Nowak GL, Bullier J. Axons, but not cell bodies, are activated by electrical stimulation in cortical gray matter II. Evidence from selective inactivation of cell bodies and axon initial segments. Experimental Brain Research. 1998b; 118(4):489–500. [PubMed: 9504844]

Nummenmaa A, McNab JA, Savadjiev P, Okada Y, Hämäläinen MS, Wang R, et al. Targeting of White Matter Tracts with Transcranial Magnetic Stimulation. Brain Stimulation. 2014; 7(1):80–84. [PubMed: 24220599]

Nummenmaa A, Stenroos M, Ilmoniemi RJ, Okada YC, Hämäläinen MS, Raij T. Comparison of spherical and realistically shaped boundary element head models for transcranial magnetic stimulation navigation. Clinical Neurophysiology. 2013; 124(10):1995–2007. [PubMed: 23890512]

Opitz A, Legon W, Rowlands A, Bickel WK, Paulus W, Tyler WJ. Physiological observations validate finite element models for estimating subject-specific electric field distributions induced by transcranial magnetic stimulation of the human motor cortex. NeuroImage. 2013; 81:253–264. [PubMed: 23644000]

Opitz A, Windhoff M, Heidemann RM, Turner R, Thielscher A. How the brain tissue shapes the electric field induced by transcranial magnetic stimulation. NeuroImage. 2011; 58(3):849–859. [PubMed: 21749927]

Ott G, Wrba J, Lucke R. Recent developments of Mn–Zn ferrites for high permeability applications. Journal of Magnetism and Magnetic Materials. 2003; 254–255:535–537.

Paffi A, Camera F, Carducci F, Rubino G, Tampieri P, Liberti M, et al. A Computational Model for Real-Time Calculation of Electric Field due to Transcranial Magnetic Stimulation in Clinics. International Journal of Antennas and Propagation. 2015:976854.

Palstra TTM, Batlogg B, van Dover RB, Schneemeyer LF, Waszczak JV. Critical currents and thermally activated flux motion in high-temperature superconductors. Applied Physics Letters. 1989; 54(8):763–765.

Pascual-Leone A, Houser CM, Reese K, Shotland LI, Grafman J, Sato S, et al. Safety of rapid-rate transcranial magnetic stimulation in normal volunteers. Clinical Neurophysiology. 1993; 89(2): 120–130.

Peasgood W, Dissado LA, Lam CK, Armstrong A, Wood W. A novel electrical model of nerve and muscle using Pspice. Journal of Physics D: Applied Physics. 2003; 36(4):311.

Pechmann A, Delvendahl I, Bergmann TO, Ritter C, Hartwigsen G, Gleich B, et al. The number of full-sine cycles per pulse influences the efficacy of multicycle transcranial magnetic stimulation. Brain Stimulation. 2012; 5(2):148–154. [PubMed: 22037129]

Peterchev AV, D'Ostilio K, Rothwell JC, Murphy DL. Controllable pulse parameter transcranial magnetic stimulator with enhanced circuit topology and pulse shaping. J Neural Eng. 2014; 11(5):056023. [PubMed: 25242286]

Peterchev AV, D'Ostilio K, Rothwell JC, Murphy DL. Controllable pulse parameter transcranial magnetic stimulator with enhanced circuit topology and pulse shaping. Journal of Neural Engineering. 2014; 11(5):056023. [PubMed: 25242286]

Peterchev, AV., Deng, Z-D., Goetz, SM. Advances in transcranial magnetic stimulation technology. In: Reti, IM., editor. Brain Stimulation: Methodologies and Interventions. Hoboken, NJ: John Wiley & Sons; 2015.

Peterchev AV, Goetz SM, Westin GG, Luber B, Lisanby SH. Pulse width dependence of motor threshold and input–output curve characterized with controllable pulse parameter transcranial magnetic stimulation. Clinical Neurophysiology. 2013; 124(7):1364–1372. [PubMed: 23434439]

Peterchev AV, Jalinous R, Lisanby SH. A Transcranial Magnetic Stimulator Inducing Near-Rectangular Pulses With Controllable Pulse Width (cTMS). IEEE Transactions on Biomedical Engineering. 2008; 55(1):257–266. [PubMed: 18232369]

Peterchev AV, Murphy DL, Lisanby SH. Repetitive transcranial magnetic stimulator with controllable pulse parameters. Journal of Neural Engineering. 2011; 8(3):036016. [PubMed: 21540487]

Peterchev AV, Murphy DLK, Goetz SM. Quiet transcranial magnetic stimulation: Status and future directions. Proc IEEE Eng Biol Med Conf (EMBC). 2015; 37:226–229.

Pitcher JB, Ogston KM, Miles TS. Age and sex differences in human motor cortex input–output characteristics. The Journal of Physiology. 2003; 546(2):605–613. [PubMed: 12527746]

Polson MJR, Barker AT, Freeston IL. Stimulation of nerve trunks with time-varying magnetic fields. Medical and Biological Engineering and Computing. 1982; 20(2):243–244. [PubMed: 7098583]

Popper, KR. The logic of scientific discovery. Oxford: Routledge; 2005.

Preisach F. Über die magnetische Nachwirkung. Zeitschrift für Physik. 1935; 94(5–6):277–302.

Rasband MN, Peles E. The Nodes of Ranvier: Molecular Assembly and Maintenance. Cold Spring Harbor Perspectives in Biology. 2016; 8(3)

Ravazzani P, Ruohonen J, Grandori F, Tognola G. Magnetic stimulation of the nervous system: Induced electric field in unbounded, semi-infinite, spherical, and cylindrical media. Annals of Biomedical Engineering. 1996; 24(5):606–616. [PubMed: 8886241]

Reilly JP. Peripheral nerve stimulation by induced electric currents: Exposure to time-varying magnetic fields. Medical and Biological Engineering and Computing. 1989; 27(2):101–110. [PubMed: 2689806]

Reilly JP. Principles of Nerve and Heart Excitation by Time-varying Magnetic Fields. Annals of the New York Academy of Sciences. 1992; 649(1):96–117. [PubMed: 1580521]

Riehl, ME. Neuronetics, Inc. System and method to reduce discomfort using nerve stimulation. US. 7,857,746. 2004.

Riehl, ME., Ghiron, KM. Neuronetics, Inc. Magnetic core for medical procedures. US. 8,657,731. 2005.

Robinson PA. Neural field theory of synaptic plasticity. Journal of Theoretical Biology. 2011; 285(1): 156–163. [PubMed: 21767551]

Rösler KM. Transcranial Magnetic Brain Stimulation: a Tool to Investigate Central Motor Pathways. Physiology. 2001; 16(6):297–302.

Rösler KM, Roth DM, Magistris MR. Trial-to-trial size variability of motor-evoked potentials. A study using the triple stimulation technique. Experimental Brain Research. 2008; 187(1):51–59. [PubMed: 18231784]

Rotem A, Neef A, Neef NE, Agudelo-Toro A, Rakhmilevitch D, Paulus W, et al. Solving the Orientation Specific Constraints in Transcranial Magnetic Stimulation by Rotating Fields. PLoS ONE. 2014; 9(2):e86794. [PubMed: 24505266]

Roth BJ, Basser PJ. A model of the stimulation of a nerve fiber by electromagnetic induction. IEEE Transactions on Biomedical Engineering. 1990; 37(6):588–597. [PubMed: 2354840]

Roth BJ, Maccabee PJ, Eberle LP, Amassian VE, Hallett M, Cadwell J, et al. In vitro evaluation of a 4-leaf coil design for magnetic stimulation of peripheral nerve. Electroencephalography and Clinical Neurophysiology. 1994; 93(1):68–74. [PubMed: 7511524]

Roth Y, Levkovitz Y, Pell GS, Ankry M, Zangen A. Safety and Characterization of a Novel Multi-channel TMS Stimulator. Brain Stimulation. 2014; 7(2):194–205. [PubMed: 24529836]

Roy Choudhury K, Boyle L, Burke M, Lombard W, Ryan S, McNamara B. Intra subject variation and correlation of motor potentials evoked by transcranial magnetic stimulation. Irish Journal of Medical Science. 2011; 180(4):873–880. [PubMed: 21660652]

Rudiak D, Marg E. Finding the depth of magnetic brain stimulation: a re-evaluation. Electroencephalography and Clinical Neurophysiology/Evoked Potentials Section. 1994; 93(5): 358–371.

Ruohonen J, Ilmoniemi R. Focusing and targeting of magnetic brain stimulation using multiple coils. Med Biol Eng Comp. 1998; 36(3):297–301.

Ruohonen J, Ilmoniemi RJ. Focusing and targeting of magnetic brain stimulation using multiple coils. Medical and Biological Engineering and Computing. 1998; 36(3):297–301. [PubMed: 9747568]

Ruohonen J, Karhu J. Navigated transcranial magnetic stimulation. Neurophysiologie Clinique/Clinical Neurophysiology. 2010; 40(1):7–17. [PubMed: 20230931]

Ruohonen J, Ravazzani P, Grandori F. Functional magnetic stimulation: theory and coil optimization. Bioelectrochem Bioenerg. 1998; 47(2):213–219.

Ruohonen J, Ravazzani P, Grandori F, Ilmoniemi RJ. Theory of multichannel magnetic stimulation: toward functional neuromuscular rehabilitation. IEEE Transactions on Biomedical Engineering. 1999; 46(6):646–651. [PubMed: 10356871]

Ruohonen J, Ravazzani P, Nilsson J, Panizza M, Grandori F, Tognola G. A volume-conduction analysis of magnetic stimulation of peripheral nerves. IEEE Transactions on Biomedical Engineering. 1996; 43(7):669–678. [PubMed: 9216138]

Ruohonen J, Virtanen J, Ilmoniemi RJ. Coil optimization for magnetic brain stimulation. Annals of Biomedical Engineering. 1997; 25(5):840–849. [PubMed: 9300108]

Rush S, Driscoll DA. Current distribution in the brain from surface electrodes. Anesth Anal. 1968; 47(6):717–723.

Rusu CV, Murakami M, Ziemann U, Triesch J. A Model of TMS-induced I-waves in Motor Cortex. Brain Stimulation. 2014; 7(3):401–414. [PubMed: 24680789]

Sahlsten H, Isohanni J, Haapaniemi J, Salonen J, Paavola J, Löyttyniemi E, et al. Electric field navigated transcranial magnetic stimulation for chronic tinnitus: A pilot study. Int J Audiol. 2015; 54(12):899–909. [PubMed: 26086944]

Salinas FS, Lancaster JL, Fox PT. 3D modeling of the total electric field induced by transcranial magnetic stimulation using the boundary element method. Physics in Medicine and Biology. 2009; 54(12):3631. [PubMed: 19458407]

Salvador R, Miranda PC, Roth Y, Zangen A. High-Permeability Core Coils for Transcranial Magnetic Stimulation of Deep Brain Regions. Proc IEEE Eng Biol Med Conf EMBC. 2007; 29:6652–6655.

Salvador R, Silva S, Basser PJ, Miranda PC. Determining which mechanisms lead to activation in the motor cortex: a modeling study of transcranial magnetic stimulation using realistic stimulus waveforms and sulcal geometry. Clinical Neurophysiol. 2011a; 122(4):748–758.

Salvador R, Silva S, Basser PJ, Miranda PC. Determining which mechanisms lead to activation in the motor cortex: A modeling study of transcranial magnetic stimulation using realistic stimulus waveforms and sulcal geometry. Clinical Neurophysiology. 2011b; 122(4):748–758. [PubMed: 21035390]

Sawicki B, Starzynski J, Wincenciak S. Numerical model of magnetic stimulation with metal implants. IEEE Transactions on Magnetics. 2006; 42(4):783–786.

Schmid M, Weyh T, Meyer BU. Entwicklung, Optimierung und Erprobung neuer Geräte für die magnetomotorische Stimulation von Nervenfasern/Development, Optimization and Testing of New Devices for Magnetomotive Nerve Fibre Stimulation. Biomedizinische Technik/Biomedical Engineering. 1993; 38(12):317–324. [PubMed: 8123772]

Scholz A, Reid G, Vogel W, Bostock H. Ion channels in human axons. Journal of Neurophysiology. 1993; 70(3):1274–1279. [PubMed: 7693885]

Schwarz JR, Reid G, Bostock H. Action potentials and membrane currents in the human node of Ranvier. Pflügers Archiv. 1995; 430(2):283–292. [PubMed: 7675638]

Scott AC. The electrophysics of a nerve fiber. Reviews of Modern Physics. 1975; 47(2):487–533.

Sekino M, Ueno S. Comparison of current distributions in electroconvulsive therapy and transcranial magnetic stimulation. Journal of Applied Physics. 2002; 91(10):8730–8732.

Sekino M, Ueno S. FEM-based determination of optimum current distribution in transcranial magnetic stimulation as an alternative to electroconvulsive therapy. IEEE Transactions on Magnetics. 2004; 40(4):2167–2169.

Senoussi S. Review of the critical current densities and magnetic irreversibilities in high Tc superconductors. Journal de Physique III. 1992; 2(7):1041–1257.

Shokrollahi H, Janghorban K. Soft magnetic composite materials (SMCs). Journal of Materials Processing Technology. 2007; 189(1–3):1–12.

Siebner HR, Peller M, Willoch F, Auer C, Bartenstein P, Drzezga A, et al. Imaging functional activation of the auditory cortex during focal repetitive transcranial magnetic stimulation of the primary motor cortex in normal subjects. Neuroscience Letters. 1999; 270(1):37–40. [PubMed: 10454140]

Silva S, Basser PJ, Miranda PC. Elucidating the mechanisms and loci of neuronal excitation by transcranial magnetic stimulation using a finite element model of a cortical sulcus. Clinical Neurophysiology. 2008; 119(10):2405–2413. [PubMed: 18783986]

Soleimani M, Lionheart WRB, Peyton AJ, Xiandong M, Higson SR. A three-dimensional inverse finite-element method applied to experimental eddy-current imaging data. IEEE Transactions on Magnetics. 2006; 42(5):1560–1567.

Sommer M, Ciocca M, Hannah R, Hammond P, Neef N, Paulus W, et al. Intermittent theta burst stimulation inhibits human motor cortex when applied with mostly monophasic (anterior-posterior) pulses. Clinical Neurophysiology. 2014; 125(1):S228.

Sommer M, D'Ostilio K, Ciocca M, Hannah R, Hammond P, Goetz S, et al. TMS can selectively activate and condition two different sets of excitatory synaptic inputs to corticospinal neurones in human. SFN Society for Neuroscience. 2014:542.

Sommer M, Lang N, Tergau F, Paulus W. Neuronal tissue polarization induced by repetitive transcranial magnetic stimulation? NeuroReport. 2002; 13(6):809–811. [PubMed: 11997692]

Sommer M, Norden C, Schmack L, Rothkegel H, Lang N, Paulus W. Opposite Optimal Current Flow Directions for Induction of Neuroplasticity and Excitation Threshold in the Human Motor Cortex. Brain Stimulation. 2013; 6(3):363–370. [PubMed: 22885142]

Starck J, Rimpiläinen I, Pyykkö I, Esko T. The Noise Level in Magnetic Stimulation. Scandinavian Audiology. 1996; 25(4):223–226. [PubMed: 8975992]

Starzynski J, Szmurlo R, Sawicki B. Distributed Optimization Environment for Bioelectromagnetism. Theoretical Engineering (ISTET). 2009; 15:1–5.

Stenfelt S, Goode RL. Bone-Conducted Sound: Physiological and Clinical Aspects. Otology & Neurotology. 2005; 26(6):1245–1261. [PubMed: 16272952]

Stephanova DI, Bostock H. A distributed-parameter model of the myelinated human motor nerve fibre: temporal and spatial distributions of action potentials and ionic currents. Biological Cybernetics. 1995; 73(3):275–280. [PubMed: 7548315]

Suárez-Bagnasco D, Armentano-Feijoo R, Suárez-Ántola. The excitation functional for magnetic stimulation of fibers. Proc IEEE Conf EMBS. 2010:4829–4833.

Szecsi J, Götz S, Pöllmann W, Straube A. Force–pain relationship in functional magnetic and electrical stimulation of subjects with paresis and preserved sensation. Clinical Neurophysiology. 2010; 121(9):1589–1597. [PubMed: 20382558]

Szlavik, RB. Nicotinic Acetylcholine Receptor Kinetics of the Neuromuscular Junction Simulated Using SPICE: An Illustration of Physiological Process Simulation with Conventional Circuit Simulation Software. Proceedings of the 2008 ASEE Annual Conference and Exposition; 2008.

Szlavik RB, Bhuiyan AK, Carver A, Jenkins F. Neural-electronic inhibition simulated with a neuron model implemented in SPICE. IEEE Transactions on Neural Systems and Rehabilitation Engineering. 2006; 14(1):109–115. [PubMed: 16562638]

Szlavik RB, de Bruin H. The effect of stimulus current pulse width on nerve fiber size recruitment patterns. Medical Engineering & Physics. 1999; 21(6–7):507–515. [PubMed: 10624746]

Tachas NJ, Samaras T. The effect of head and coil modeling for the calculation of induced electric field during transcranial magnetic stimulation. International Journal of Psychophysiology. 2014; 93(1): 167–171. [PubMed: 23872490]

Takada Y, Abe M, Masuda S, Inagaki J. Commercial scale production of Fe-6.5 wt. % Si sheet and its magnetic properties. Journal of Applied Physics. 1988; 64(10):5367–5369.

Tang AD, Makowiecki K, Bartlett C, Rodger J. Low intensity repetitive transcranial magnetic stimulation does not induce cell survival or regeneration in a mouse optic nerve crush model. PLoS One. 2015; 10(5):e0126949. [PubMed: 25993112]

Thielscher A, Kammer T. Linking physics and physiology in TMS: a sphere field model to determine the cortical stimulation site in TMS. Neuroimage. 2002; 17(3):1117–1130. [PubMed: 12414254]

Thielscher A, Opitz A, Windhoff M. Impact of the gyral geometry on the electric field induced by transcranial magnetic stimulation. NeuroImage. 2011; 54(1):234–243. [PubMed: 20682353]

Thomas SL, Gorassini MA. Increases in Corticospinal Tract Function by Treadmill Training After Incomplete Spinal Cord Injury. Journal of Neurophysiology. 2005; 94(4):2844–2855. [PubMed: 16000519]

Tixador P, Porcar L, Floch E, Buzon D, Isfort D, Bourgault D, et al. Current limitation with bulk Y-Ba-Cu-O. IEEE Transactions on Applied Superconductivity. 2001; 11(1):2034–2037.

Tofts PS. The distribution of induced currents in magnetic stimulation of the nervous system. Physics in Medicine and Biology. 1990; 35(8):1119–1128. [PubMed: 2217537]

Toschi N, Keck ME, Welt T, Guerrisi M. Quantifying uncertainty in Transcranial Magnetic Stimulation – A high resolution simulation study in ICBM space. Proc IEEE Eng Biol Med Conf EMBC. 2012; 34:1218–1221.

Toschi N, Welt T, Guerrisi M, Keck ME. A reconstruction of the conductive phenomena elicited by transcranial magnetic stimulation in heterogeneous brain tissue. Physica Medica. 2008; 24(2):80–86. [PubMed: 18296093]

Toschi N, Welt T, Guerrisi M, Keck ME. Transcranial magnetic stimulation in heterogeneous brain tissue: Clinical impact on focality, reproducibility and true sham stimulation. Journal of Psychiatric Research. 2009; 43(3):255–264. [PubMed: 18514227]

Treutwein B, Strasburger H. Fitting the psychometric function. Perception & Psychophysics. 1999; 61(1):87–106. [PubMed: 10070202]

Trimmer JS, Rhodes KJ. Localization of Voltage-Gated Ion Channels IN Mammalian Brain. Annual Review of Physiology. 2004; 66(1):477–519.

Tringali S, Perrot X, Collet L, Moulin A. Repetitive transcranial magnetic stimulation: Hearing safety considerations. Brain Stimulation. 2012; 5(3):354–363. [PubMed: 21824837]

Turner R. A target field approach to optimal coil design. Journal of Physics D: Applied Physics. 1986; 19(8):L147.

Ueno S, Tashiro T, Harada K. Localized stimulation of neural tissues in the brain by means of a paired configuration of time-varying magnetic fields. Journal of Applied Physics. 1988a; 64(10):5862–5864.

Ueno S, Tashiro T, Harada K. Localized stimulation of neural tissues in the brain by means of a paired configuration of time-varying magnetic fields. J Appl Phys. 1988b; 64(10):5862–5864.

Uglietti D, Yanagisawa Y, Maeda H, Kiyoshi T. Measurements of magnetic field induced by screening currents in YBCO solenoid coils. Superconductor Science and Technology. 2010; 23(11):115002.

Ursino M, Cona F, Zavaglia M. The generation of rhythms within a cortical region: Analysis of a neural mass model. NeuroImage. 2010; 52(3):1080–1094. [PubMed: 20045071]

Vacher H, Trimmer JS. Trafficking mechanisms underlying neuronal voltage-gated ion channel localization at the axon initial segment. Epilepsia. 2012; 53:21–31. [PubMed: 23216576]

van Kuijk AA, Anker LC, Pasman JW, Hendriks JCM, van Elswijk G, Geurts ACH. Stimulus–response characteristics of motor evoked potentials and silent periods in proximal and distal upper-extremity muscles. Journal of Electromyography and Kinesiology. 2009; 19(4):574–583. [PubMed: 18396413]

van Kuijk AA, Pasman JW, Hendricks HT, Zwarts MJ, Geurts ACH. Predicting Hand Motor Recovery in Severe Stroke: The Role of Motor Evoked Potentials in Relation to Early Clinical Assessment. Neurorehabilitation and Neural Repair. 2009; 23(1):45–51. [PubMed: 18794218]

Volz LJ, Hamada M, Rothwell JC, Grefkes C. What Makes the Muscle Twitch: Motor System Connectivity and TMS-Induced Activity. Cerebral Cortex. 2014; 25(9):2346–2353. [PubMed: 24610120]

Wagner T, Eden U, Fregni F, Valero-Cabre A, Ramos-Estebanez C, Pronio-Stelluto V, et al. Transcranial magnetic stimulation and brain atrophy: a computer-based human brain model study. Experimental Brain Research. 2008; 186(4):539–550. [PubMed: 18193208]

Wagner T, Eden U, Rushmore J, Russo CJ, Dipietro L, Fregni F, et al. Impact of brain tissue filtering on neurostimulation fields: A modeling study. NeuroImage. 2014; 85(3):1048–1057. [PubMed: 23850466]

Wagner TA, Zahn M, Grodzinsky AJ, Pascual-Leone A. Three-dimensional head model simulation of transcranial magnetic stimulation. IEEE Transactions on Biomedical Engineering. 2004; 51(9): 1586–1598. [PubMed: 15376507]

Wang X, Chen Y, Guo M, Wang M. Design of Multi-channel Brain Magnetic Stimulator and ANSYS Simulation. International Journal of Bioelectromagnetism. 2005; 7(1):259–262.

Wang X, Wang J, Deng B, Wei X-l, Li HY. The effects of induction electric field on sensitivity of firing rate in a single-compartment neuron model. Neurocomputing. 2013; 99:555–563.

Wassermann EM, Zimmermann T. Transcranial magnetic brain stimulation: Therapeutic promises and scientific gaps. Pharmacology & Therapeutics. 2012; 133(1):98–107. [PubMed: 21924290]

Weissman JD, Epstein CM, Davey KR. Magnetic brain stimulation and brain size: relevance to animal studies. Electroencephalogr Clin Neurophysiol. 1992; 85(3):215–219. [PubMed: 1376680]

Wilson MT, Goodwin DP, Brownjohn PW, Shemmell J, Reynolds JNJ. Numerical modelling of plasticity induced by transcranial magnetic stimulation. Journal of Computational Neuroscience. 2014; 36(3):499–514. [PubMed: 24150916]

Windhoff M, Opitz A, Thielscher A. Electric field calculations in brain stimulation based on finite elements: An optimized processing pipeline for the generation and usage of accurate individual head models. Human Brain Mapping. 2013; 34(4):923–935. [PubMed: 22109746]

Wolf EW, Walker CF. Design And Practical Considerations In The Construction Of Magnetic Induction Stimulators. Proc IEEE Eng Biol Med Conf EMBC. 1991; 13:857–858.

Wong SH, Cendes ZJ. Numerically stable finite element methods for the Galerkin solution of eddy current problems. IEEE Transactions on Magnetics. 1989; 25(4):3019–3021.

Wongsarnpigoon A, Warren MG. Energy-efficient waveform shapes for neural stimulation revealed with a genetic algorithm. Journal of Neural Engineering. 2010; 7(4):046009. [PubMed: 20571186]

Wongsarnpigoon A, Woock JP, Grill WM. Efficiency Analysis of Waveform Shape for Electrical Excitation of Nerve Fibers. Neural Systems and Rehabilitation Engineering, IEEE Transactions on. 2010; 18(3):319–328.

Xiong H, Shi JH, Hu XW, Liu JZ. The Focusing Optimization of Transcranial Magnetic Stimulation System. Progress In Electromagnetics Research. 2016; 48:145–154.

Xu G, Wang M, Chen Y, Yang S, Yan W. The Optimal Design of Magnetic Coil in Transcranial Magnetic Stimulation. Proc IEEE Conf EMBS. 2005; 27:6221–6224.

Yamaguchi M, Yamada S, Daimon N, Yamamoto I, Kawakami T, Takenaka T. Electromagnetic mechanism of magnetic nerve stimulation. Journal of Applied Physics. 1989; 66(3):1459–1465.

Yang, S., Xu, G., Wang, L., Chen, Y., Wu, H., Li, Y., et al. 3D realistic head model simulation based on transcranial magnetic stimulation. 2006, Aug. 30 2006-Sept. 3 2006; Paper presented at the Engineering in Medicine and Biology Society, 2006. EMBS '06. 28th Annual International Conference of the IEEE;

Yang S, Xu G, Wang L, Geng Y, Yu H, Yang Q. Circular Coil Array Model for Transcranial Magnetic Stimulation. IEEE Transactions on Applied Superconductivity. 2010; 20(3):829–833.

Zangen A, Roth Y, Voller B, Hallett M. Transcranial magnetic stimulation of deep brain regions: evidence for efficacy of the H-Coil. Clinical Neurophysiology. 2005; 116(4):775–779. [PubMed: 15792886]

Zarkowski P, Shin CJ, Dang T, Russo J, Avery D. EEG and the Variance of Motor Evoked Potential Amplitude. Clinical EEG and Neuroscience. 2006; 37(3):247–251. [PubMed: 16929713]

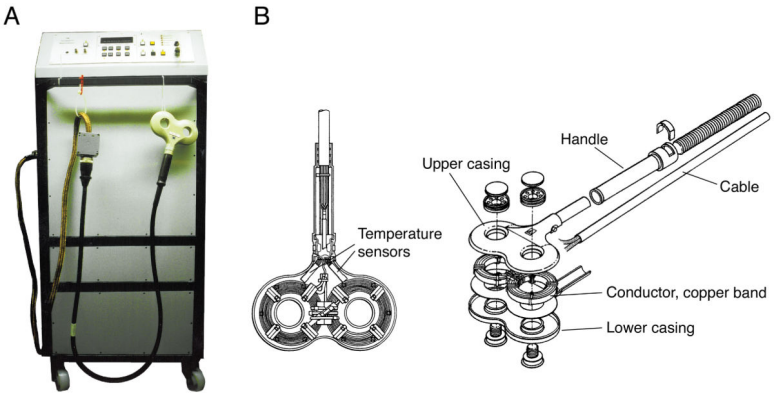

Figure 1.

A. Early repetitive stimulators such as the depicted monophasic stimulator with maximum repetition rates of more than 30 Hz, peak voltage of 5,000 V, and variable rise-time provided by adjustable capacitance between 40 μF and 200 μF allowed neuromuscular magnetic stimulation in the periphery and neuromodulatory protocols in the brain for the first time (Schmid, et al., 1993). B. Structure of a modern figure-of-eight coil, which is typically formed by a conductor loop, here a copper band, between the two pieces of the casing. The coil incorporates at least one, often two temperature sensors near the conductor that terminate stimulation when the coil exceeds the safe temperature range. It is usually filled with hardening resin for mechanical robustness, thermal conductivity, and electrical safety (modified from (Mould, 1998)).

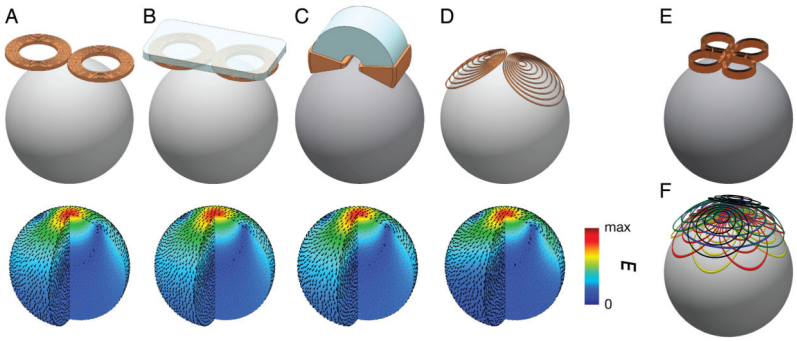

Figure 2.

Example illustrations of TMS coils (top) and the corresponding induced electric field distributions simulated in a spherical model (bottom). A. 70-mm figure-of-eight coil (The Magstim Ltd., Whitland, Wales). B. Figure-of-eight coil with soft-magnetic back-plate. C. C-core coil (Neuronetics, Inc., Malvern, PA). D. Minimum energy eccentric coil (Knäulein & Weyh, 1996). E. Cloverleaf coil. F. Multi-focal multi-layer coil, composed of two orthogonal layers of cloverleaf coils, a circular coil, and two orthogonal layers of figure-8 coils.

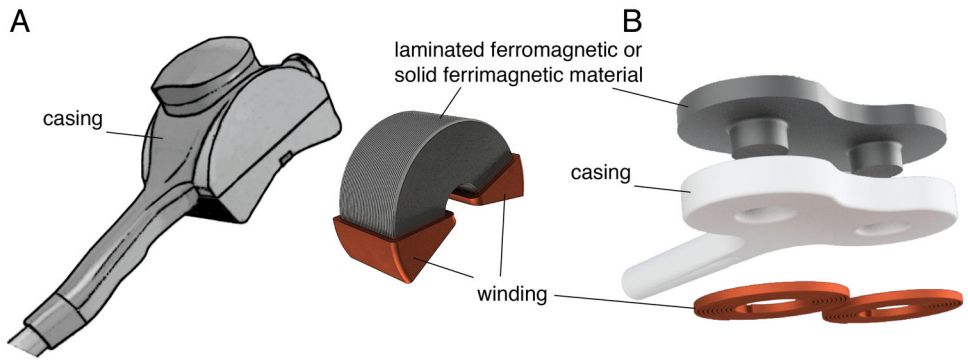

Figure 3.

Different approaches for improving stimulation coils with soft-magnetic materials: A. Commercial C-core coil (Neuronetics, Inc., Malvern, PA) and B. core-enhanced figure-of-eight coil with magnetic back-plate to reduce the field energy of the field as presented by A. Barker (A. T. Barker, 2001).

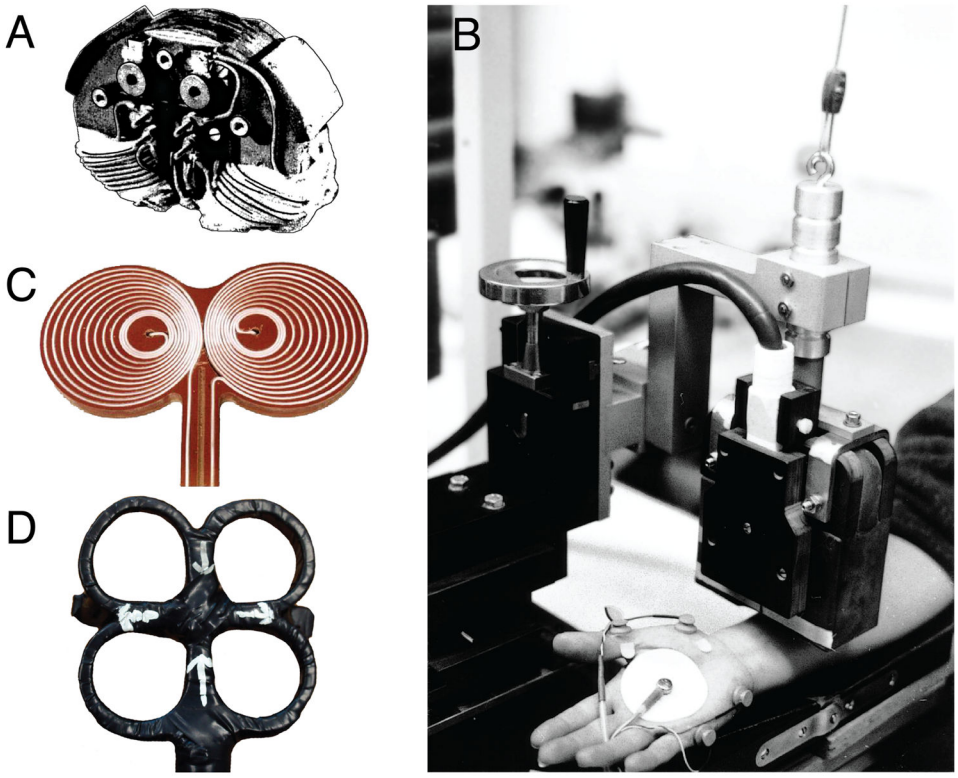

Figure 4.

Actual implementations of early magnetic stimulation coils: A. and B. early academic coils with C-shaped cores of a cobalt-steel alloy with high permeability and saturation level (Lorenzen & Weyh, 1992; Schmid, et al., 1993) (Courtesy of Dr. Thomas Weyh). C. Eccentric figure-of-eight coil. D. Cloverleaf coil (Courtesy of Dr. Eric Wassermann).

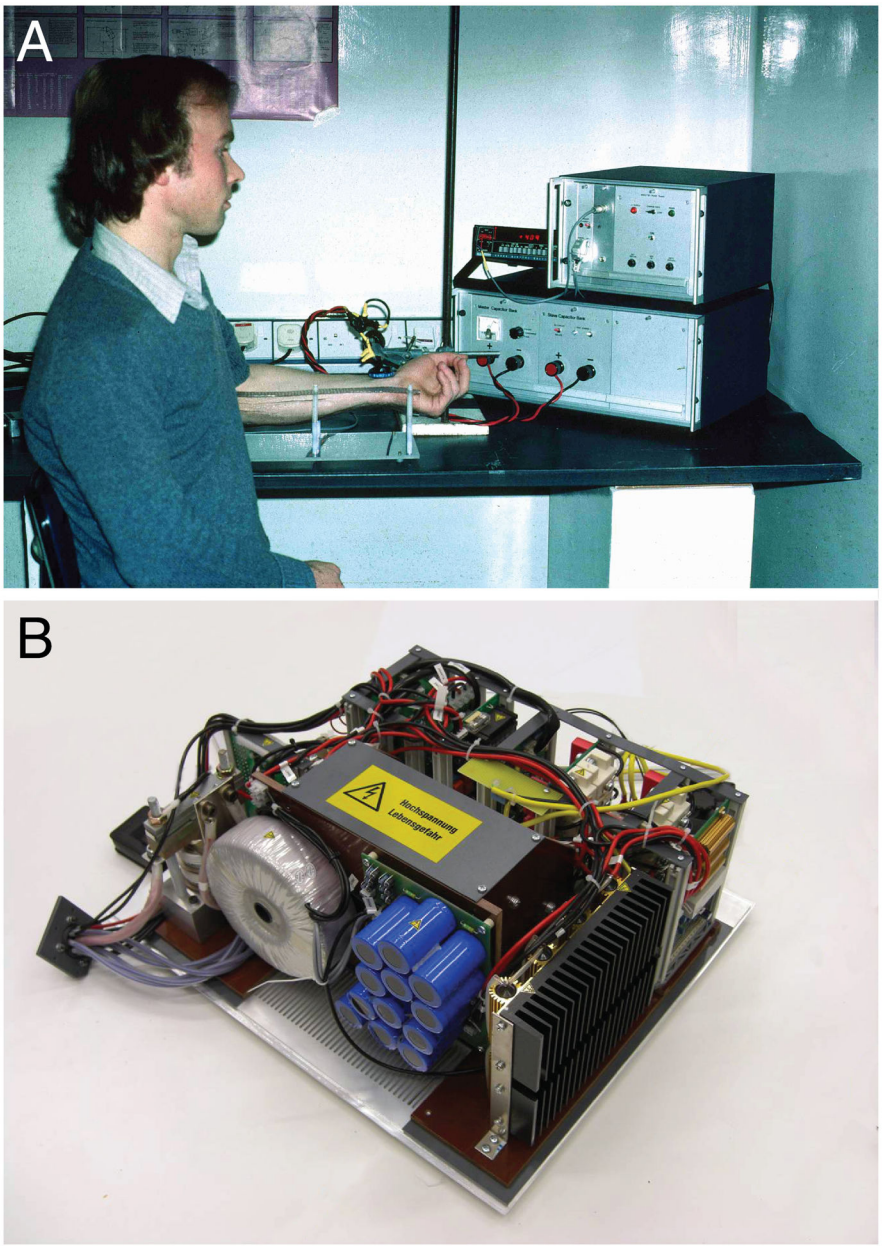

Figure 5.

A. First magnetic stimulator built by Drs. M. Polson and A. Barker in 1982, which was a single-pulse device primarily tested in animals and peripherally (Polson, et al., 1982) (Courtesy of Dr. Michael Polson). B. Modern repetitive pulse source with power supply, high-voltage pulse train, and control unit (Mag&More GmbH, Munich, Germany).

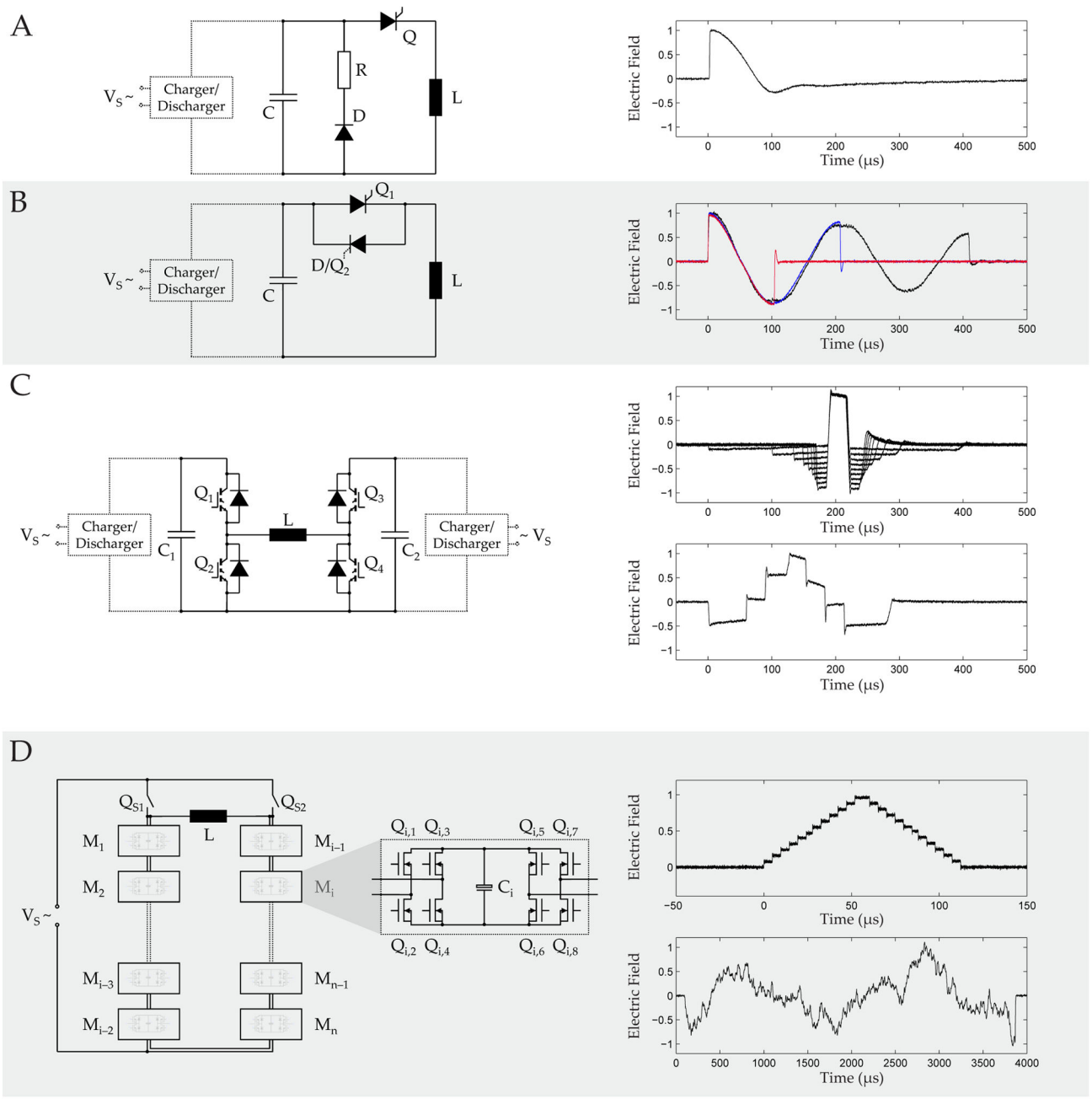

Figure 6.

Circuit topologies (left column) and typical pulse shapes (right column) of typical magnetic stimulation pulse sources. A. Monophasic stimulator, B. Biphasic and polyphasic stimulator, C. controllable parameter TMS (cTMS), D. Modular pulse synthesizer.

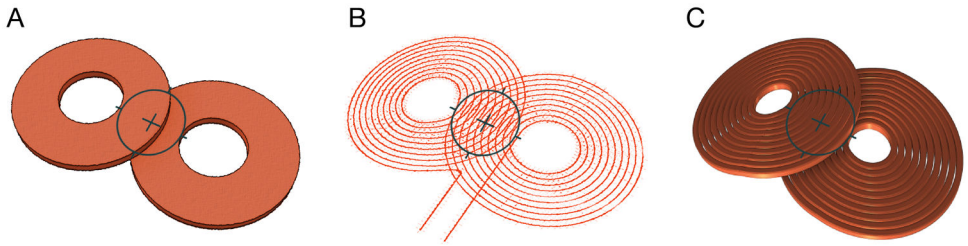

Figure 7.

Coil models with: A. bulk conductor, B. individual turns with idealized line current, and C. individual turns with 3D representation of windings, demonstrating the increasing level of detail in induced-field modeling.

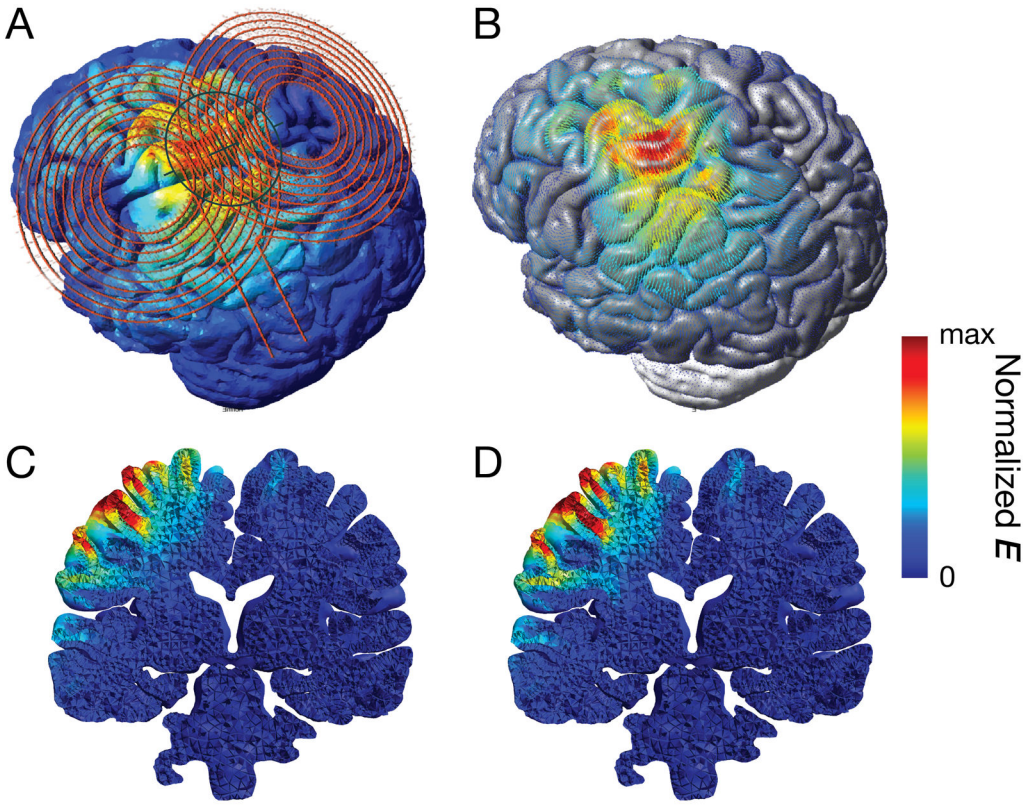

Figure 8.

Realistic head model of TMS: A. Figure-of-eight coil placed over the left primary motor cortex. B. Induced electric field distribution showing the effect of a focus spread out over several gyri. C. A coronal view at the level of the TMS hotspot, in a head model that assumes isotropic tissue conductivity for the white matter. D. The same view as in C in a head model that incorporated white matter anisotropy derived from diffusion tensor imaging data. The model shows slightly deeper reach of the electric field.

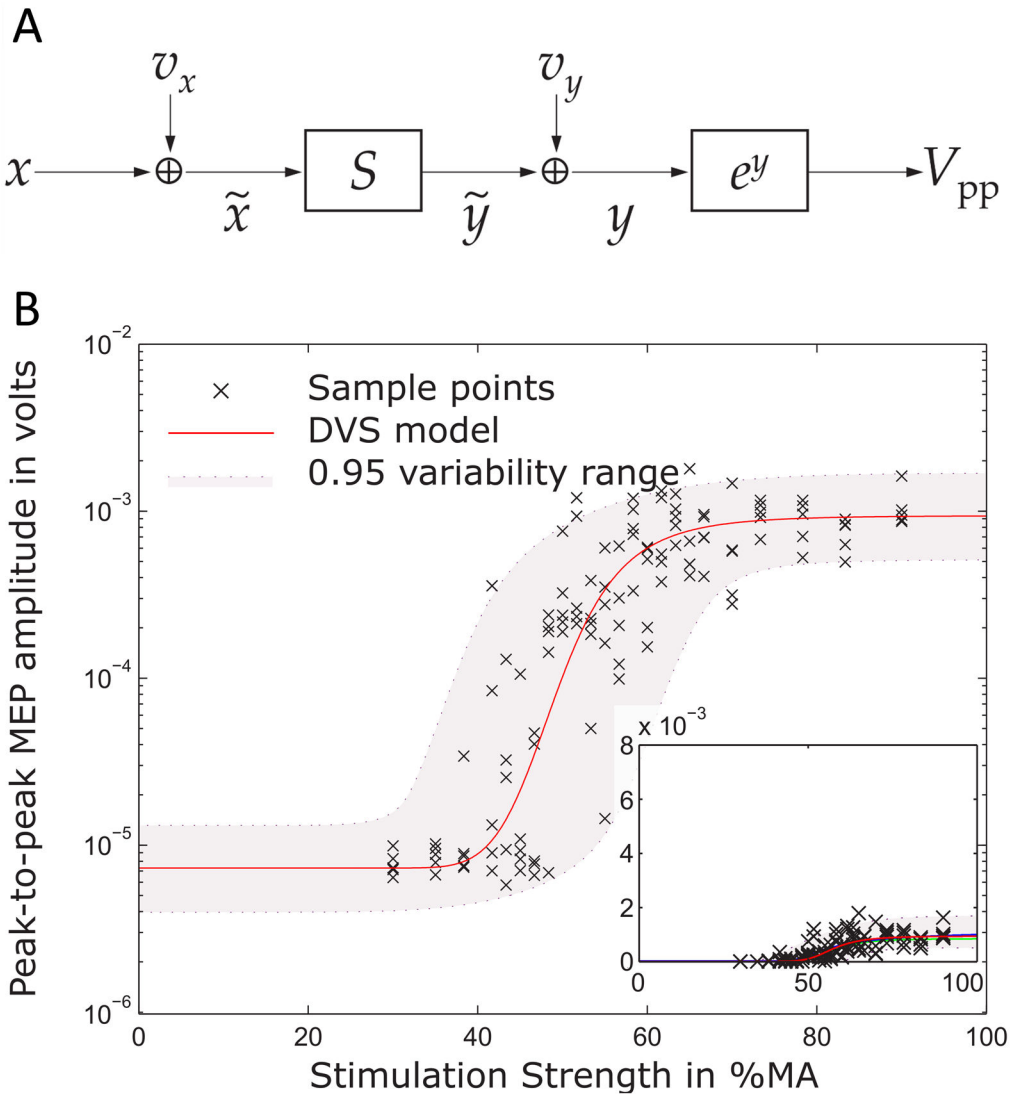

Figure 9.

Model for describing the stimulus–response behavior of motor-evoked potentials. A. Each stimulus with strength x that activates the motor cortical target is perturbed by a variability source v_x, which describes ongoing endogenous neuromodulation and incoming signals to the activated neurons. A summation S represents the recruitment of the many parallel units. A second variability source v_y and an exponential function together describe the multiplicative output-side variability, which is caused by effects in the periphery, such as cellular fluctuations of calcium concentrations and fatigue, and measurement noise. B. The model (line and grey band) well describes the experimental behavior given by the crosses and allows splitting variability into its contributions to detect endogenous neuromodulation of the stimulated neurons in real-time.